ARMY RESEARCH LABORATORY

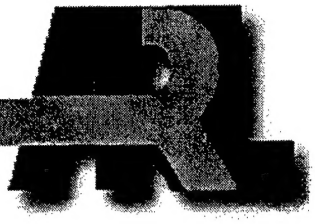

Aerodynamics of the 120-mm M831A1 Projectile: Analysis of Free Flight Experimental Data

Keith P. Soencksen
James F. Newill
Peter Plostins

ARL-TR-2307 NOVEMBER 2000

Approved for public release; distribution is unlimited.

The findings in this report are not to be construed as an official Department of the Army position unless so designated by other authorized documents.

Citation of manufacturer's or trade names does not constitute an official endorsement or approval of the use thereof.

Destroy this report when it is no longer needed. Do not return it to the originator.

Army Research Laboratory
Aberdeen Proving Ground, MD 21005-5066

ARL-TR-2307 November 2000

Aerodynamics of the 120-mm M831A1 Projectile: Analysis of Free Flight Experimental Data

Keith P. Soencksen
James F. Newill
Peter Plostins
Weapons & Materials Research Directorate

Abstract

The 120-mm M831A1 projectile is a low-cost training projectile used by U.S. armor troops. For the last several years, program managers have received feedback from the users that in some cases, M831A1 impact performance did not appear consistent with the current M831A1 computer correction factor. Based on this information, a low-scale but in-depth experimental analysis of the projectile was conducted to assess its aero-ballistic qualities and hopefully identify any potential issues that could affect accuracy performance. The work was conducted by the U.S. Army Research Laboratory at the Transonic Experimental Facility. Although the projectile has undergone fairly extensive target impact dispersion (TID), radar, and wind tunnel testing, this study presents the first spark range data and detailed free-flight aero-ballistic analysis for the M831A1.

Roll data were measured via roll pins for the computation of roll-related coefficients. All rounds exhibited very little roll over the measured trajectory, mostly because of a very small roll moment. Yaw magnitudes displayed variability, and several shots had at least moderate levels. The source of the yaw levels imparted to the projectiles was the launch dynamics, and a detailed study of in-bore dynamics is in progress. Most shots exhibited a "stepping" motion in plots of total yaw versus range. This phenomenon is the result of trim, which is believed to be caused by an aerodynamic asymmetry. A source of the trim has not been isolated. Accurate free-flight drag and pitching moment coefficients were computed on the basis of the measured trajectories. Pitch-damping characteristics were marginal.

Although the M831A1 currently performs within acceptable TID standards, further experimental work is recommended, as well as a study of possible stabilizer design modifications.

ACKNOWLEDGMENTS

The authors would like to thank the U.S. Army Operations Support Command (formerly the Industrial Operations Command) for funding this work. The U.S. Army Research, Development, and Engineering Center (ARDEC) at Picatinny Arsenal, New Jersey, provided much support and guidance. We especially recognize the contributions of Mr. John Kostka, Mr. Leon Manole, and Mr. Anthony Farina of ARDEC. We also acknowledge Alliant Techsystems for supplying all projectile hardware and Arrowtech Associates for providing valuable technical support.

INTENTIONALLY LEFT BLANK

Contents

Figures

Tables

AERODYNAMICS OF THE 120-MM M831A1 PROJECTILE: ANALYSIS OF FREE FLIGHT EXPERIMENTAL DATA

1. Introduction

The 120-mm M831A1 projectile is a low-cost training projectile used by U.S. armor troops. The M831A1 training ammunition program is managed by the U.S. Army Operations Support Command (OSC), formerly the Industrial Operations Command (IOC), at Rock Island, Illinois, which is supported by the U.S. Army Research, Development, and Engineering Center (ARDEC) at Picatinny Arsenal, New Jersey. The M831A1 is used as a surrogate training round for high explosive, antitank (HEAT) M830 and M830A1 service rounds. In 1994, the M831A1 replaced the M831 projectile, which had been produced and used as a training round until then. The M831A1 resulted in significant cost savings for the Government since the boom and fins of the M831 were replaced with a simple slotted stabilizer. Today, the round is produced by two Government contractors, each producing approximately 50% of the rounds purchased by the Army. A photograph of the M831A1 is shown in Figure 1, and a schematic is shown in Figure 2.

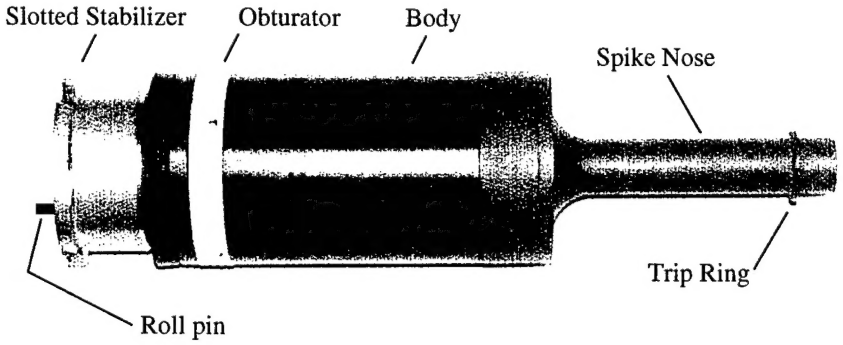

Figure 1. 120-mm M831A1 Training Projectile.

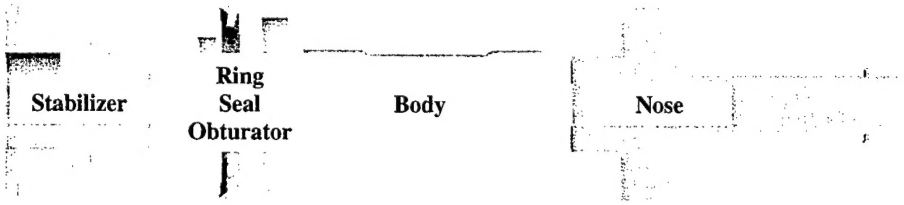

Figure 2. Schematic of the 120-mm M831A1 Training Projectile.

The M831A1 is fired annually in large numbers from the M1A1 tank by training armor crews. As with all projectile types, a computer correction factor (CCF) or "fleet zero" is used in the tank's fire control system to account for average fleet projectile jump. For the last several years, OSC (IOC) has received feedback from the users that in some cases, M831A1 impact performance did not appear consistent with the current M831A1 CCF. Based on this information, the IOC and ARDEC sought a low-scale but in-depth analysis of the projectile to assess its aero-ballistic qualities and hopefully identify any potential issues that could affect accuracy performance. Recently, IOC funded a separate, extensive experimental firing program to study the M865E3 kinetic energy (KE) training projectile at the Transonic Experimental Facility (TEF) of the U.S. Army Research Laboratory (ARL), Aberdeen Proving Ground, Maryland. In order to maximize cost benefit, it was decided to fire five M831A1 projectiles during the same experiment in an attempt to address the issues described previously and to obtain at least a preliminary look at its free flight behavior. Alliant Techsystems manufactured and provided all the projectiles used in the experiment.

Although the projectile has undergone fairly extensive target impact dispersion (TID), radar, and wind tunnel evaluation, the data acquired from the current experiment are significant since they represent the first spark range data and detailed aero-ballistic analysis of the M831A1.

2. Setup and Methodology

The experiment was fired from an M1A1 main battle tank with a 120-mm M256 gun system (tube serial number 3700). All five rounds were fired through the TEF's spark range facility which contains 25 orthogonal shadowgraph stations. An interior view of the range is shown in Figure 3.

Roll history was measured with a roll pin, which is a small pin inserted in the base of the projectile (see Figure 1). The pin is visible in each shadowgraph. Measurements of the position of the pin in each shadowgraph are used to derive the roll history, allowing for the calculation of the static roll moment coefficient and roll-damping coefficient. These coefficients are then prescribed in the 6-degree-of-freedom (DOF) motion analysis to improve the accuracy of determining other aerodynamic coefficients.

Aero-ballistic flight qualities are described by the set of aerodynamic coefficients. These were calculated via the Aero-ballistic Research Facility Data Analysis System (ARFDAS) code written and supported by Arrowtech Associates. This code uses an inverse routine that fits the measured projectile angle and position data first to the linearized equations of motion and then to the full 6-DOF

equations of motion; the code then computes the aerodynamic forces and moments required to produce the measured flight. The code also supports a multiple fit capability that allows the computation of a single set of aerodynamic parameters via the data from multiple shots. This allows the estimation of aerodynamic coefficients at higher confidence levels.

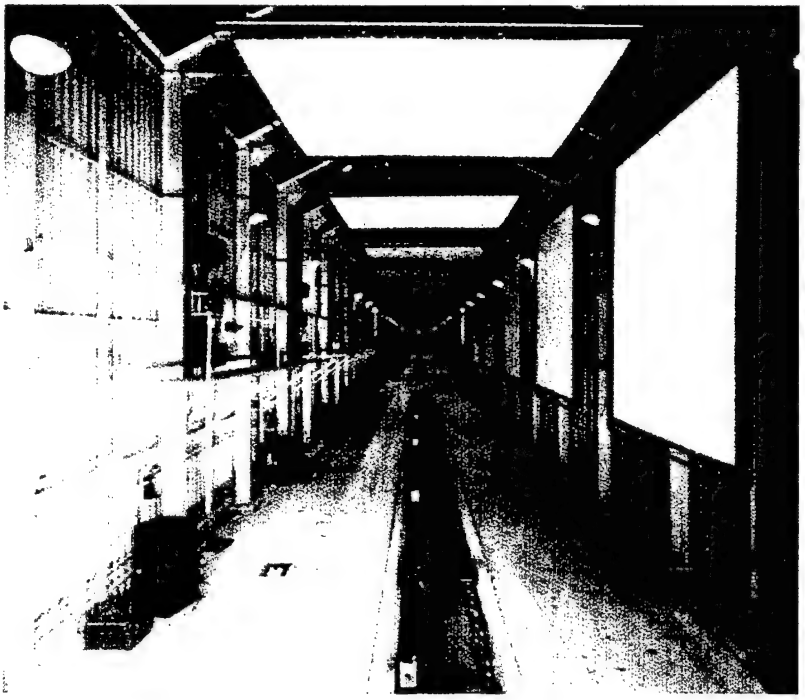

Figure 3. Interior View, Transonic Experimental Facility.

Table 1 shows cross referencing between the shot numbers as they are referred to in this report and TEF's shot numbers.

Table 1. Shot Number Reference

Shot No.	ARL TEF Shot No.
1	34668
2	34669
3	34670
4	34671
5	34672

3. Experimental Results and Analysis

3.1 Shadowgraph Data

Figures 4 and 5 show shadowgraphs of the M831A1, which are representative of those recorded from the experiment. Figure 4 shows a shadowgraph that captures the M831A1 at low angle of attack. From this, we see the basic flow field encountered by the projectile, including the shock pattern and boundary layer. Shocks emanating from the tripping ring and body shoulder coalesce with the bow shock down stream. Note that the tripping ring creates a region of turbulence that grows in diameter until it approximately intersects with the body shoulder. A similar view is depicted in Figure 5, this time showing the asymmetrical flow field encountered at a moderate angle of attack (4.4 degrees). Note the large separated region of turbulence and the absence of a clearly defined shoulder shock on the leeward side of the projectile. Finally, Figure 6 shows the projectile at high angle of attack (8.2 degrees). Here, the shoulder shock is again evident on the leeward side, although it appears somewhat masked by the turbulence.

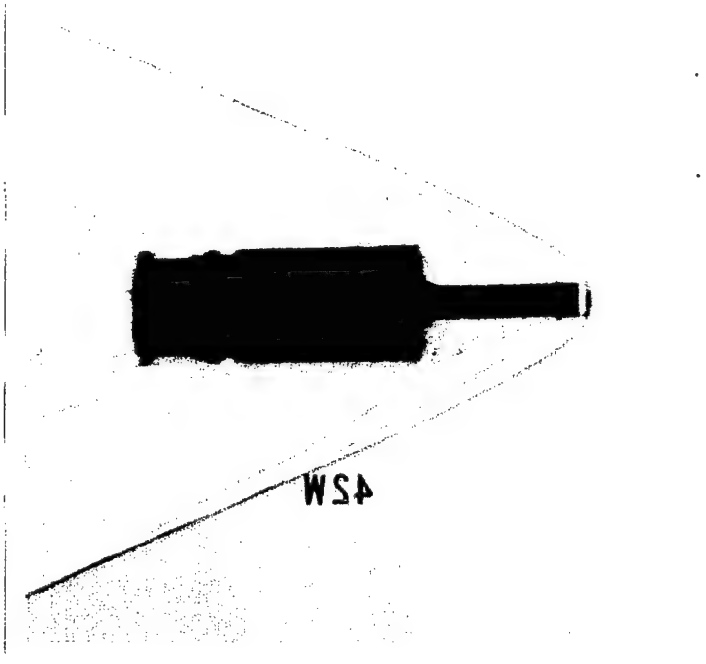

Figure 4. Shadowgraph, Shot 2, 181 meters, M = 3.1, Angle = 0.2 degree.

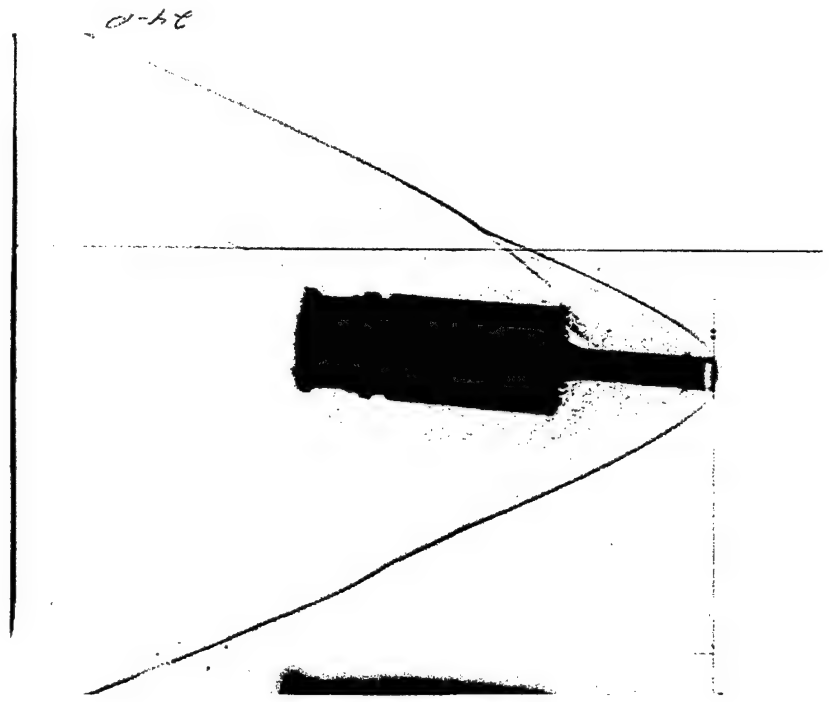

Figure 5. Shadowgraph, Shot 2, 102 meters, M = 3.1, Angle = 4.4 degrees.

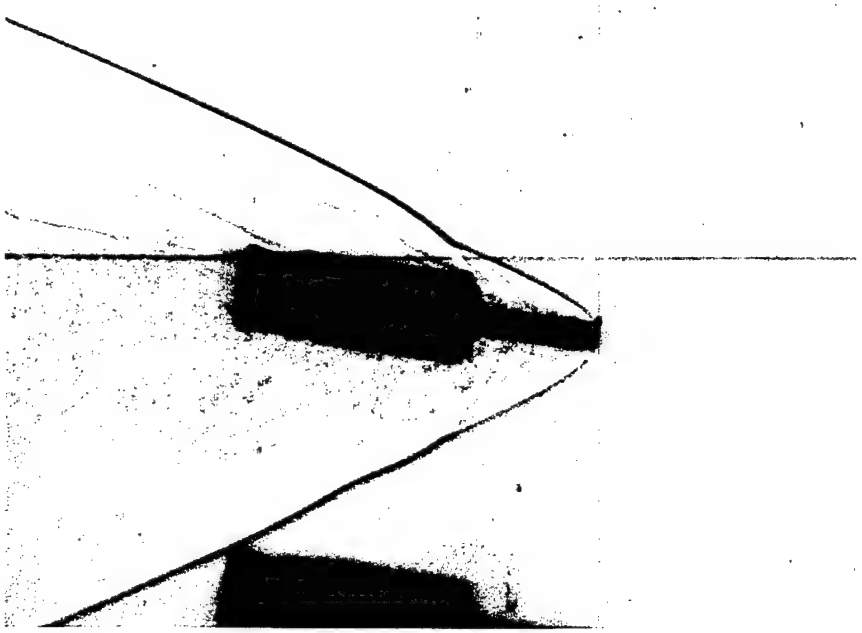

Figure 6. Shadowgraph, Shot 2, 90 meters, M = 3.1, Angle = 8.2 degrees

3.2 Roll Data

The M831A1 is a statically stable projectile. Fins are traditionally employed on most statically stable projectiles. Here, the combination of a slotted stabilizer and a spike nose provides static stability. The slots in the stabilizer are driving surfaces that provide roll torque. For a statically stable projectile, the round's roll history must be such that the effects of roll-yaw resonance are minimized and that any vehicle asymmetries will not bias the flight path. Spin rate control is a critical design feature needed to minimize the effect of small mass or configurational asymmetries.

Measuring roll history via the use of roll pins has been successfully implemented on numerous projectile types and sizes in experiments spanning the last several decades. Accurate measurement of a projectile's roll orientation is often critical to an accurate assessment of the other aerodynamic flight attributes since these attributes are all tied together in the full 6-DOF equations of motion. Although a fairly significant amount of wind tunnel roll data are available, there are few existing free flight roll data for the M831A1 (Hathaway 1999; Dohrn 1999; Durkin 1999). In 1994, Whyte, Hathaway, and Groth measured M831A1 free flight roll via the use of Doppler radar and a slotted tracer plug. One conclusion from this work was that M831A1 roll acceleration was possibly inadequate, potentially leading to occasional roll-yaw "lock-in." These facts intensified the desire for accurate measurement of free flight roll characteristics.

The roll pin survived launch on all five projectiles. However, upon inspection of the shadowgraph data, only a few displayed evidence of the pin. Figure 7 is a plot of the conclusive roll pin data for all five shots. From this, we can see that fairly comprehensive roll angle data were obtained for Shot 5. Only very sporadic data exist for Shots 1, 2, and 4, and no experimental roll data at all were acquired from Shot 3.

The reason for the apparent data loss is that determination of roll angle requires visibility of the roll pin in both pitch and yaw plane shadowgraphs. In the cases when data were missing, one of three conditions existed: (1) the roll pin was visible in the pitch plane but was not visible in the yaw plane, (2) the roll pin was not visible in the pitch plane but was visible in the yaw plane, or (3) the roll pin was not visible in either the pitch or the yaw plane. Further analysis showed that roll pins were visible only in certain orientations in each plane. This is detailed in Figure 8. With the roll orientation convention noted in the figure, examination of the data showed that when the roll pin was oriented between approximately 0 and 180 degrees, it was not visible in the horizontal shadowgraph. Similarly, when the roll pin was oriented between approximately 90 and 270 degrees, it was not visible in the vertical shadowgraph. When the pin was located between 90 and 180 degrees, it was not visible in either plane. The reason for these "blackout" regions is believed to be attributable to wake turbulence. In both

planes, the blackout region occurs when the pin is in the hemisphere farthest away from the film. It is hypothesized that when the pin is in these regions, the relative depth of the turbulent wake between the pin and the free stream causes the pin to be masked. This effect is exacerbated by projectile angle of attack, which can also cause partial masking of the pin.

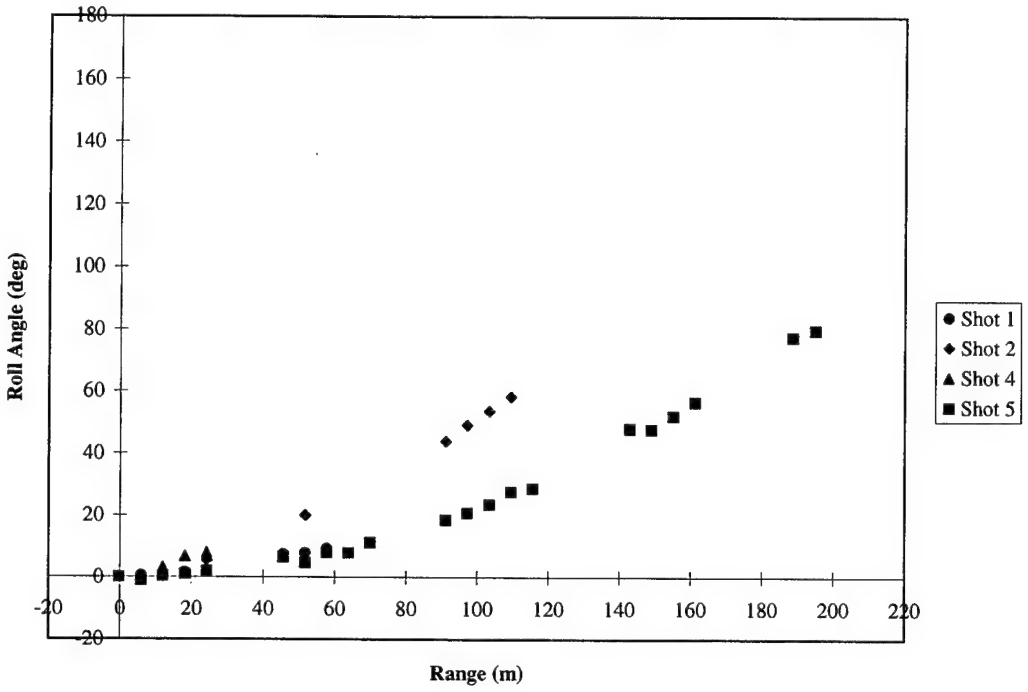

Figure 7. Roll Data as Measured Optically (standard method).

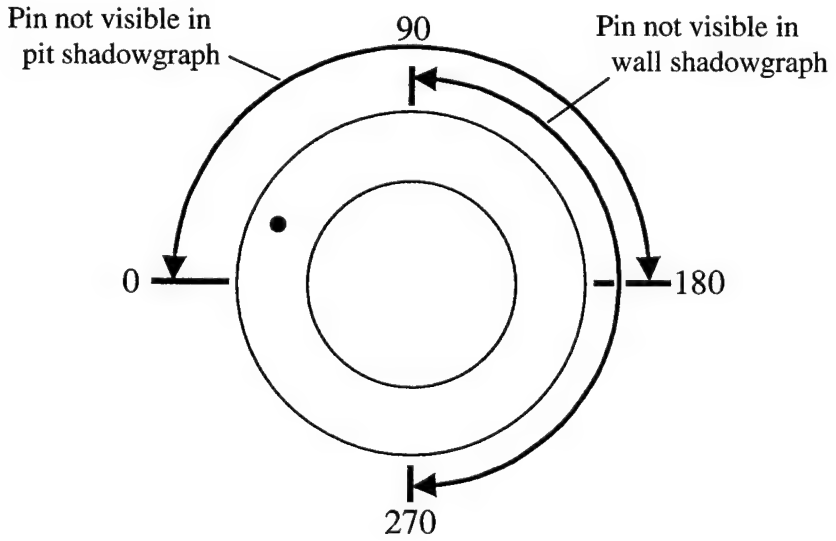

Figure 8. Roll Orientation Diagram.

Because of this, the roll data could not be analyzed by the standard optical technique, which generally yields accurate roll-related aerodynamic coefficients. However, all shadowgraphs were inspected and measured manually in order to gain further insight into the early flight spin characteristics of the M831A1. Figure 9 shows a comparison of hand-measured roll angle data versus roll angle data measured with the standard optical measurement technique for Shot 5, which contained the most comprehensive roll data. The data show very good agreement, especially given the accuracy of the hand measurements. Also, the data confirm that when the pin was oriented in the quadrant from 270 to 360 degrees, it was visible in both planes. Notice that the projectile rolled only about ¼ turn in its first 250 meters of flight.

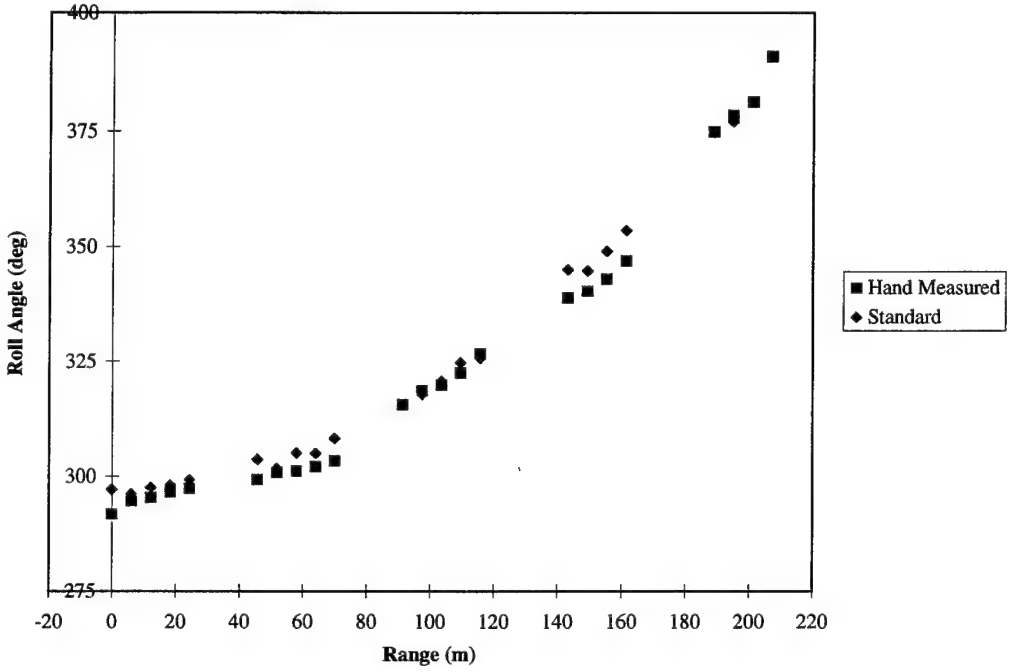

Figure 9. Shot 5 Roll Data: Hand Measurement Versus Standard Optical Measurement.

Similar measurements were performed for the other four shots. Comparisons of hand-measured roll data versus optically measured roll data are presented in Figures 10 through 13.

Figure 14 shows a plot of hand-measured roll angles for all five shots. In all shots, hand-measured data are present in some places where the standard measurement technique failed to produce data points. This was possible by simply using the hand-measured data from a single plane and inferring the correct orientation from adjacent data. The hand-measured data played a vital role in understanding the projectile roll history. In the case of Shot 3, no comparison can be made between the two measurement techniques since there are no data points from the standard measurement. For the other shots, roll angle

discrepancies were no higher than 15 to 20 degrees between the two measurement techniques. Even with such levels of discrepancy, the qualitative information obtained from the hand-measured data provides an important indication of the total amount of roll along the trajectory. It can be concluded that in all shots, the projectile rolled less than ½ revolution during its first 250 meters of flight.

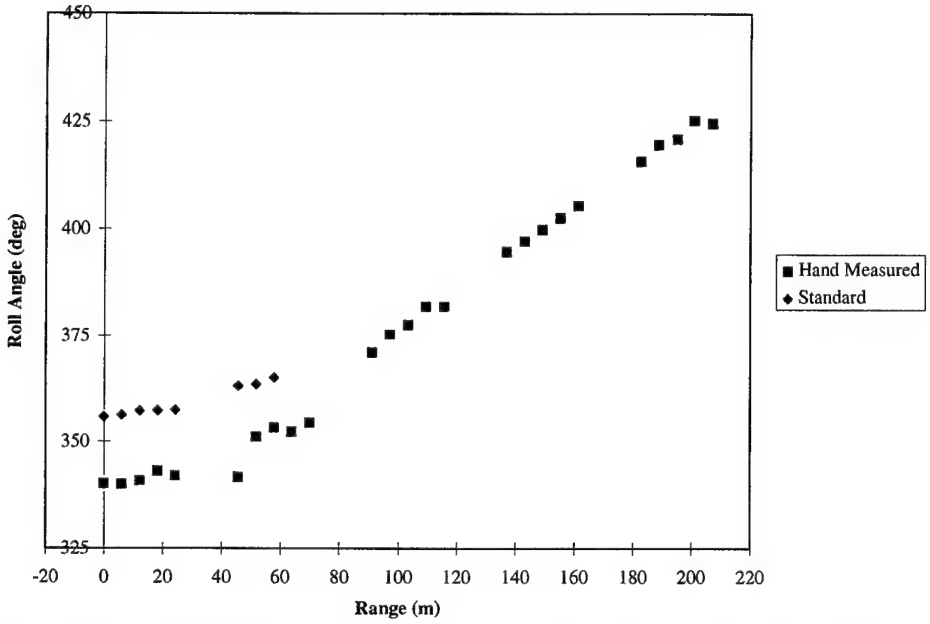

Figure 10. Shot 1 Roll Data: Hand Measurement Versus Standard Optical Measurement.

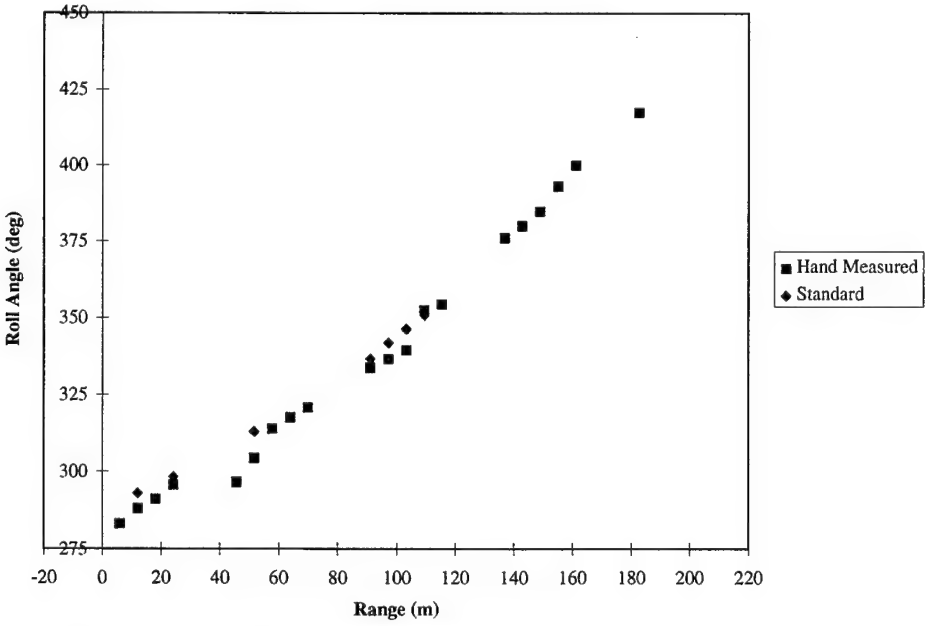

Figure 11. Shot 2 Roll Data: Hand Measurement Versus Standard Optical Measurement.

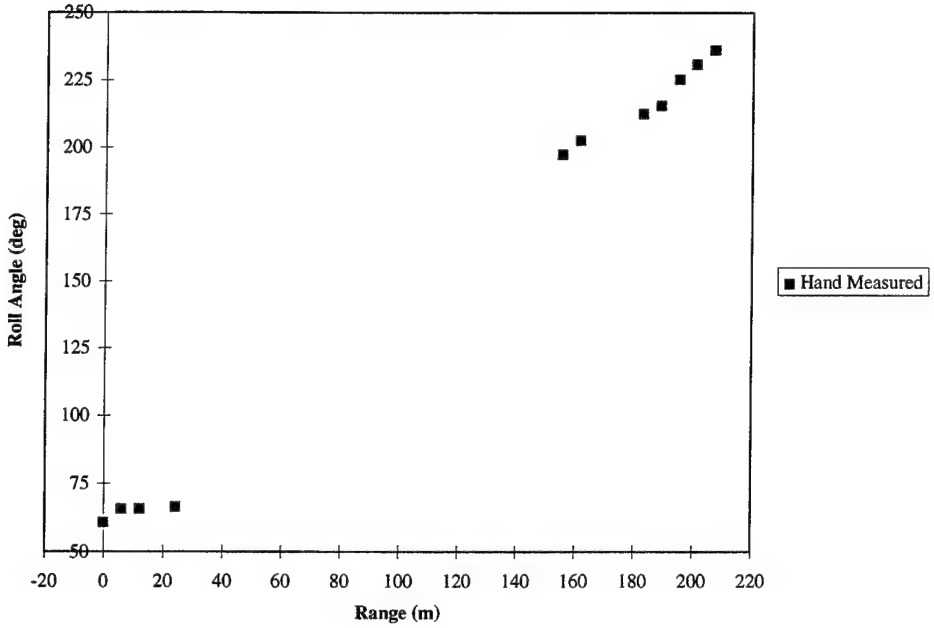

Figure 12. Shot 3 Roll Data: Hand Measurement Versus Standard Optical Measurement.

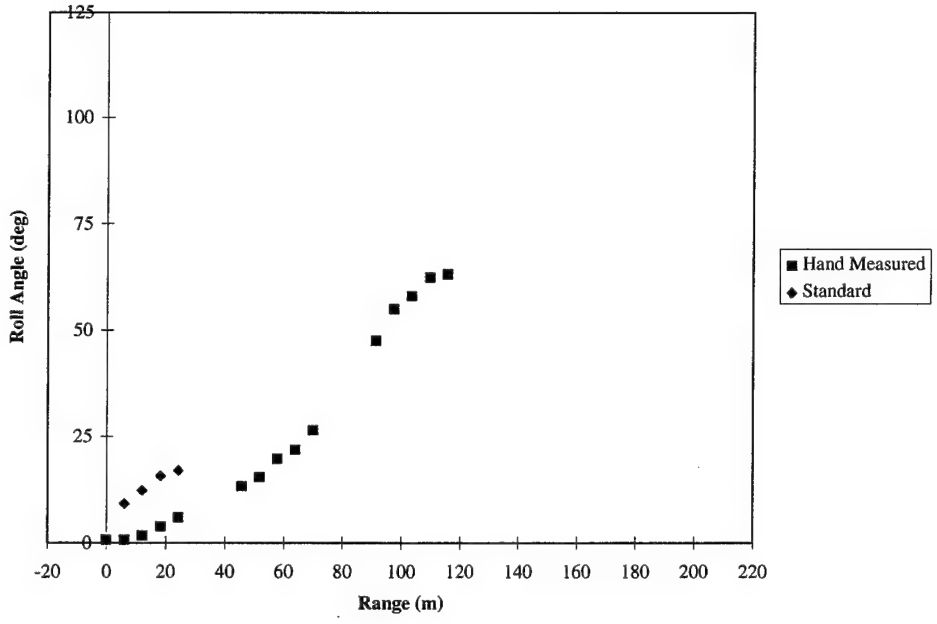

Figure 13. Shot 4 Roll Data: Hand Measurement Versus Standard Optical Measurement.

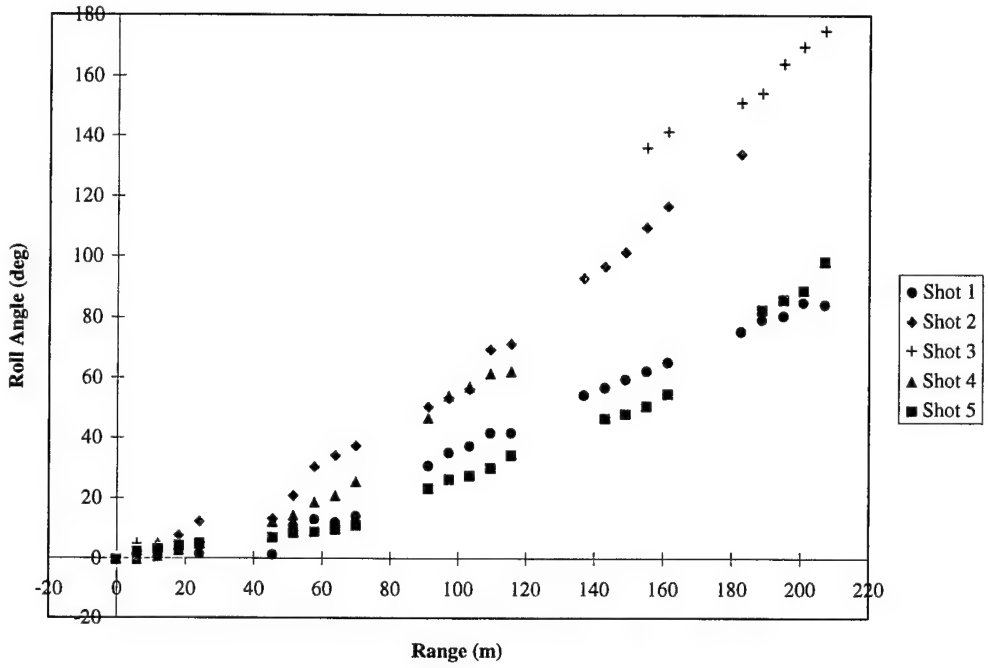

Figure 14. Hand-Measured Roll Angle Data, All Shots.

Because the spin rates are so low and so far from steady state, an accurate value for roll-damping moment coefficient ($C_{\ell p}$) is not determinable from these shots. Similarly, a good value for the static roll moment coefficient ($C_{\ell 0}$) could not be determined. However, a procedure was developed to compute a range of probable values for $C_{\ell 0}$. The procedure used the experimental data from Shot 5, which had the most populated data set. Roll data from the other four shots were too sparse for meaningful $C_{\ell 0}$ coefficient computations. First, baseline values for $C_{\ell 0}$ and $C_{\ell p}$ were obtained from the Projectile Design Analysis System (PRODAS) projectile data analysis code as 0.0024 and -0.045, respectively. These values were computed by the code, based upon analysis of a detailed projectile model coupled with accurate physical properties. When these two values were held fixed in the ARFDAS code, the program yielded a fit error of 3.3 degrees to the measured roll data. This relatively good fit error indicates that these values for $C_{\ell 0}$ and $C_{\ell p}$ are reasonable. Next, the value of $C_{\ell 0}$ was varied. That is, the baseline value for $C_{\ell p}$ (-0.045) was held fixed, and the roll fit error was computed for a range of different $C_{\ell 0}$ values. These data are depicted in Figure 15.

In this figure, the square data point represents the roll fit error (3.3 degrees) with the baseline values of $C_{\ell p}$ (-0.045) and $C_{\ell 0}$ (0.0024). As we allow $C_{\ell 0}$ to vary, we find that a $C_{\ell 0}$ of 0.0016 results in the minimum roll fit error: 1.2 degrees. Theoretically, the smaller the roll fit error, the more accurate the value of $C_{\ell 0}$. The circular data point represents the value of $C_{\ell 0}$ calculated by the ARFDAS code, given the measured roll data for Shot 5. Note that ARFDAS does an excellent job

of obtaining a value for $C_{\ell 0}$ that results in the lowest possible roll fit error. The value of $C_{\ell 0}$ computed by ARFDAS analysis is 0.00153 with a probable error in the coefficient of about 4.5%. However, given the fact that only one shot contains the required data set for such an analysis, it cannot be stated that this value is accurate for the M831A1 projectile in general. The results of this study of $C_{\ell 0}$ indicate that drawing conclusions about a probable range of values for $C_{\ell 0}$ is risky. This is because of the nature of the curve of Figure 15, which clearly shows that fairly accurate fits to measured roll data (i.e., less than 5 degrees roll fit error) are achievable with a range of $C_{\ell 0}$ values as wide as 0.0005 to 0.0026.

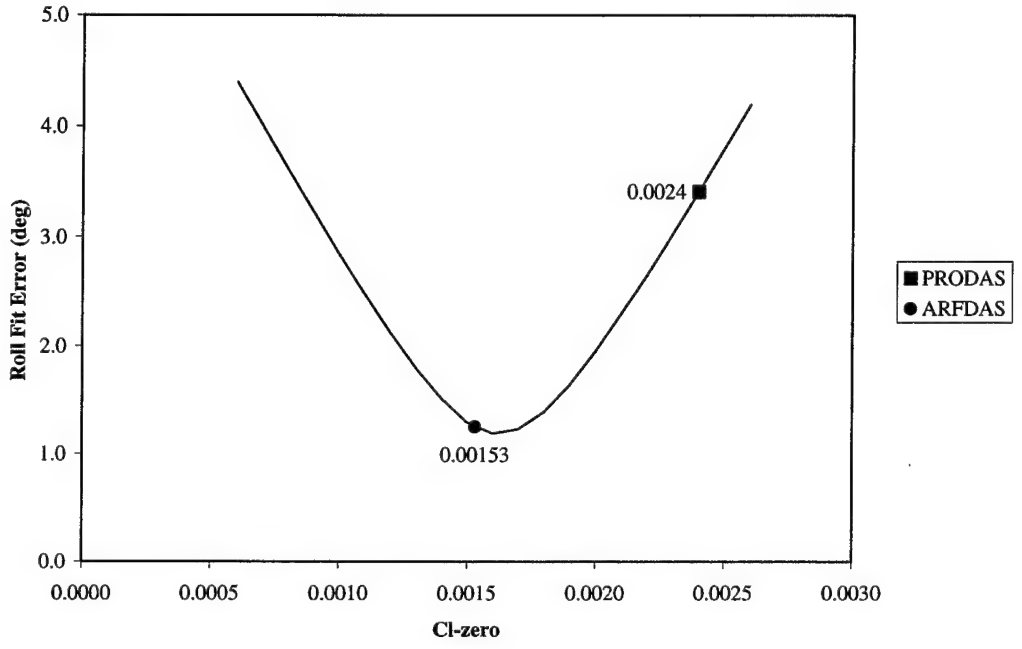

Figure 15. Roll Fit Error with Constant $C_{\ell p}$ (-0.045), Shot 5.

In an attempt to reduce the risk in estimating the proper value for $C_{\ell 0}$, another study was performed. In this analysis, the hand-measured roll data were inserted into the ARFDAS input file. All shots were then subjected to an independent data reduction, this time with the hand-measured roll data. The results of this analysis are presented in Table 2.

The general trend observed in the table is that the probable error in the $C_{\ell 0}$ computed from the hand-measured data is higher than that computed from the standard method. This is because the roll fit errors are correspondingly higher for the hand-measured data. In turn, the roll fit errors are higher because the fits of optically measured data are typically for only a few data points (except Shot 5) and thus are easier to fit with small errors. Also, the hand-measured roll fit errors are higher because of the additional variability introduced by the hand

Table 2. $C_{\ell 0}$ From Standard Measurements Versus Hand Measurements

Shot	Standard Optical Measured Roll Data				Hand-Measured Roll Data			
	Induced Roll Moment Coeff. $C_{\ell 0}$	Probable Error (percent)	Number of Stations in Roll Fit	Roll Fit Error (deg)	Induced Roll Moment Coeff. $C_{\ell 0}$	Probable Error (percent)	Number of Stations in Roll Fit	Roll Fit Error (deg)
1	0.00093	4.3	8	0.34	0.00056	30.3	24	3.74
2	0.00098	12.2	6	1.53	0.00109	15.6	15	2.8
3	--	--	0	--	--	--	11	--
4	0.00076	21.1	4	1.26	-0.00098	--	15	5.99
5	0.00153	4.6	21	1.25	0.00162	17.7	23	2.44

measurement technique itself. Despite the higher probable errors, the coefficients produced from the hand-measured data are probably more accurate than those obtained from the standard method because the number of stations used in the roll fits of hand-measured data is larger than in the standard optically measured data. Note that the hand-measured data were unable to produce meaningful values of $C_{\ell 0}$ for Shots 3 and 4. Based on this analysis, the range of probable values for $C_{\ell 0}$ can confidently be refined to between 0.0010 and 0.0016. The only way to improve this further is with more experimental roll data.

3.3 Yawing Motion

As described earlier, the position and orientation of the projectile were recorded and measured at each of the 25 orthogonal shadowgraph stations of the TEF. These data were processed and analyzed and yielded aerodynamic characteristics. Several interesting observations were gleaned from plots of the projectile yawing motion. The yawing motion in orthogonal planes is plotted in Figure 16 for Shot 1.

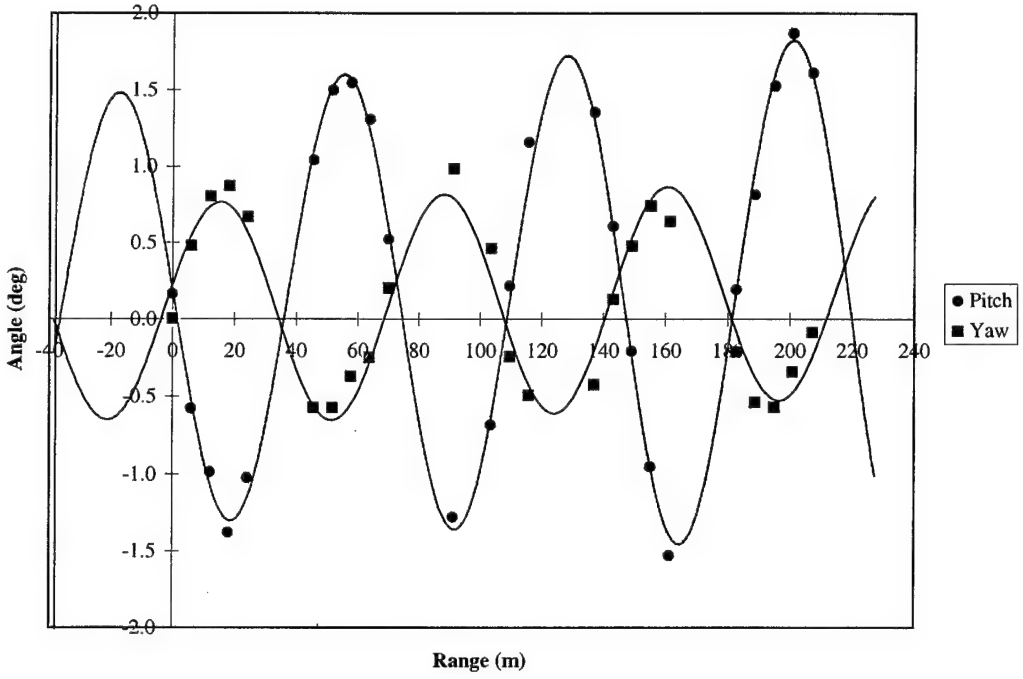

Figure 16. Pitch and Yaw Versus Range, Shot 1.

In this and subsequent yaw plots, the gun muzzle is located at -38 meters, and the sign convention is positive up and left. Shown on this plot are the experimental data points in each plane, together with the computed best fits from the full 6-DOF solution to the equations of motion. Notice that the pitch angle peaks are growing slightly with range while the yaw angle peaks appear to be approximately constant. When these angular data are combined into total angle of attack, the plot of Figure 17 results.

Here, all yaw maxima and minima are evident as far as ~220 meters. Note that the first maximum yaw (about 1.65 degrees) is greater than the second maximum yaw, as expected. The third maximum yaw, however, is greater than both the first and second maxima. In general, a slightly growing step-like pattern is displayed. A similar step-like pattern is seen when the yaw minima are examined. This is indicative of a trim angle, as described next. The magnitude of the stepping motion is possibly slightly less than that indicated by the total yaw fit. This is hypothesized because of the fit error that is inherent in any data-fitting procedure and is based on the fact that some data points are under-predicted by the fit curve. Despite the uncertainty in its exact magnitude, the stepping phenomenon of the yawing motion is definitely present and significant enough to be measurable. Evidence of this flight characteristic was also found in Shots 3, 4, and 5. Total angle of attack is plotted for these shots in Figures 19 through 21. The total angle of attack did not display any visible stepping motion in Shot 2, as shown in Figure 18. Pitch and yaw motion plots versus range for Shots 2 through 5, as well as pitch versus yaw plots for all shots are presented in the appendix. A fair amount of variability in the yaw levels from shot to shot is noted, although the sample size is small. First maximum yaw varied from less than 1 degree to more than 9 degrees for these shots.

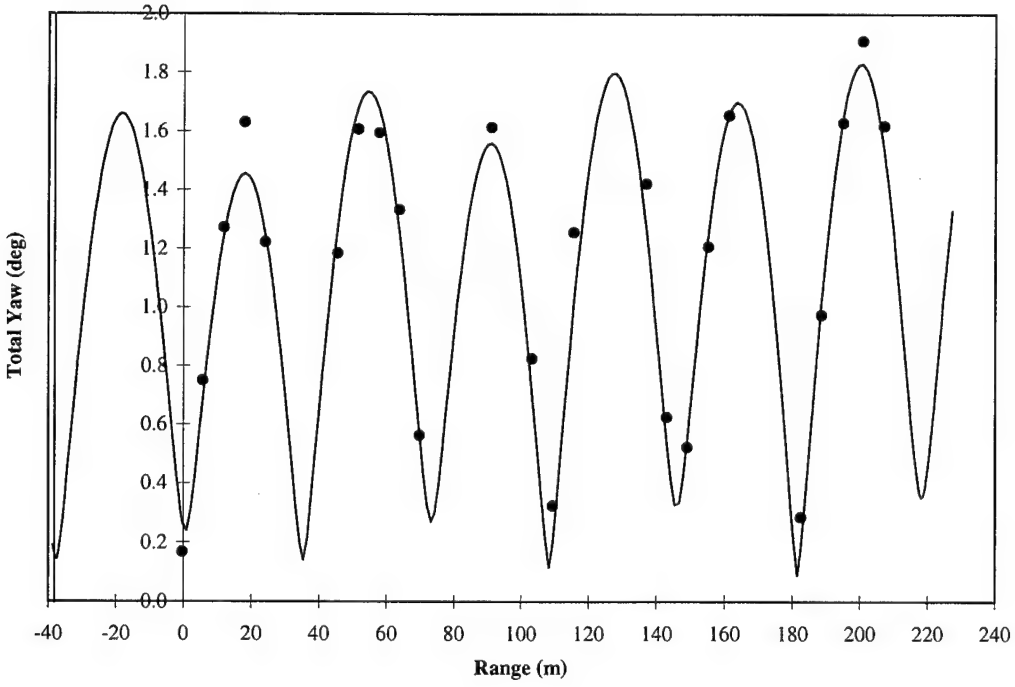

Figure 17. Total Yaw Versus Range, Shot 1.

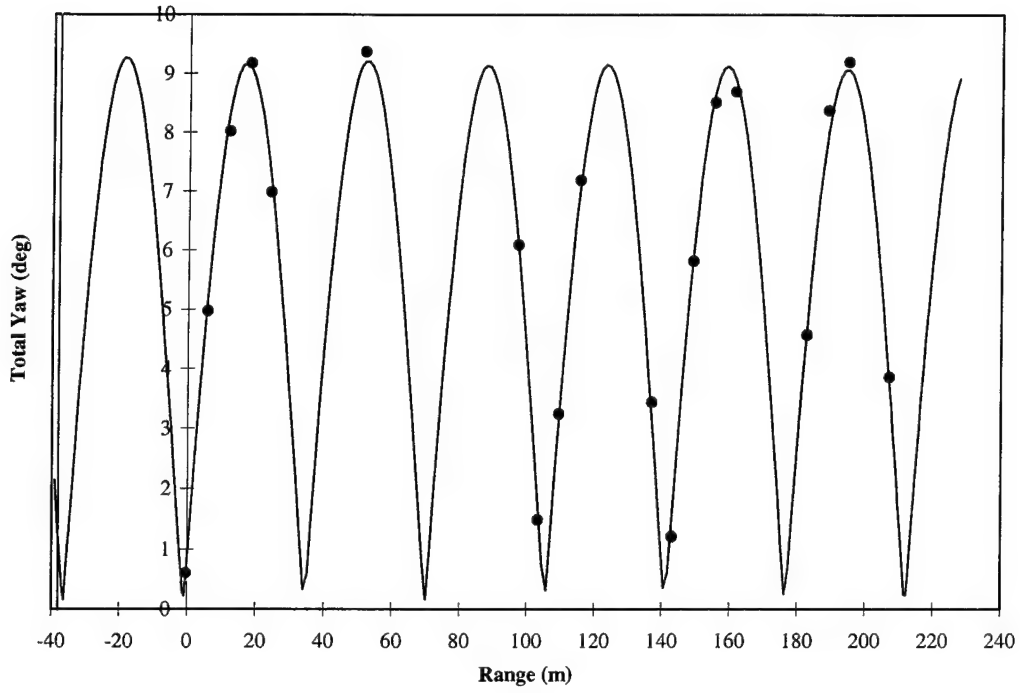

Figure 18. Total Yaw Versus Range, Shot 2.

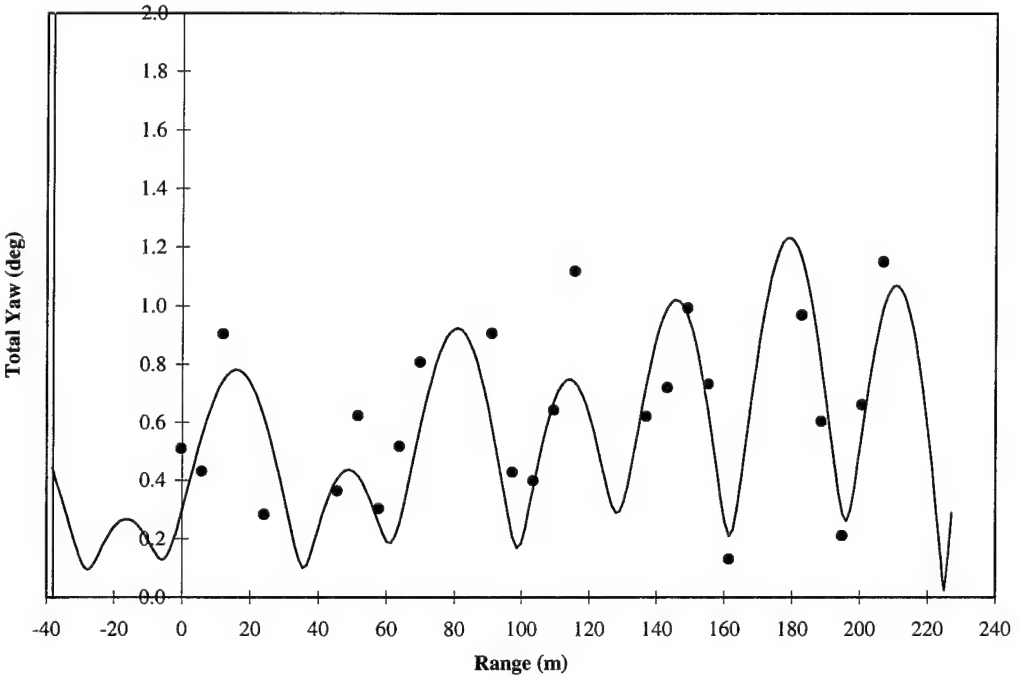

Figure 19. Total Yaw Versus Range, Shot 3.

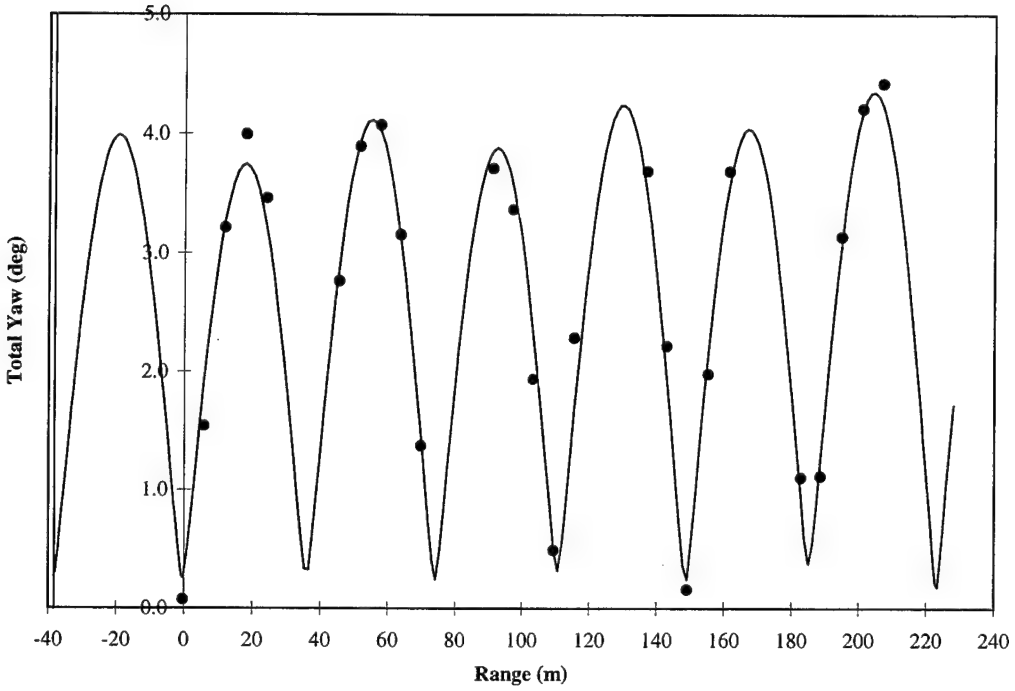

Figure 20. Total Yaw Versus Range, Shot 4.

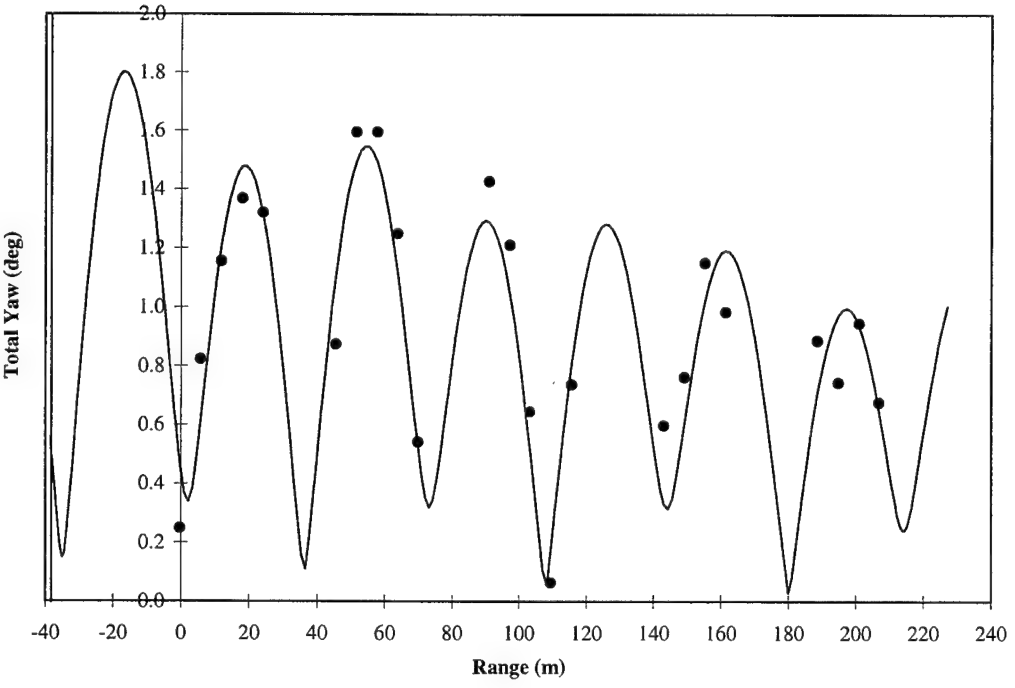

Figure 21. Total Yaw Versus Range, Shot 5.

The stepping motion observed can be explained by considering the linearized model of epicyclic projectile motion presented by Murphy (1963). This model, drawn schematically in Figure 22 for conditions at muzzle exit, is described principally by two rotating vectors, k_1 and k_2. The vectors represent the magnitudes of the fast and slow modes of yawing motion, which are theoretically equal and opposite for a statically stable projectile with no roll. The k_1 vector rotates counterclockwise (when one is looking down range) and is fixed to the origin at its base, while the k_2 vector rotates clockwise about the tip of the k_1 vector. The directions of vector rotation are indicated with arrows in Figure 22. Fast and slow mode yaw frequencies are represented in the model by the rotation rates of the two vectors. A third vector, k_3, is added when any trim forces or moments are present. In Figure 22, the k_3 vector, or *trim* vector, is illustrated pointing up, but this is arbitrary.

Note that the vector sum is not precisely zero at the muzzle. This is simply because of measurement error. According to Murphy's model, the trim vector rotates about the tip of the k_2 vector at the projectile roll rate. For rolling, statically stable projectiles with very small asymmetries, the effect of trim on the motion is usually not measurable.

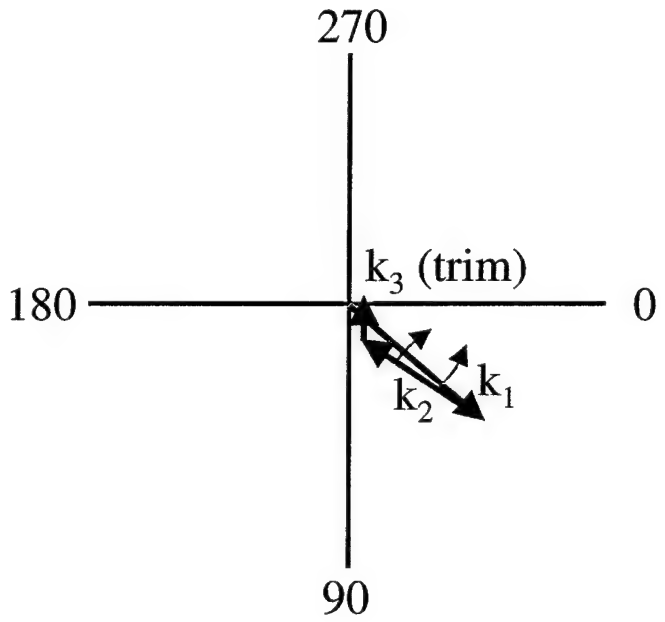

Figure 22. Tricyclic Motion Model With Arbitrary Conditions at Muzzle.

For all the M831A1 shots, roll rates were extremely low. On average, the projectile rolled about 120 degrees (1/3 revolution) in 210 meters. Although the roll profile is growing nonlinearly, assume, for simplicity, a constant roll rate of approximately 0.6 degree per meter. This means that in one full yaw period (approximately 75 meters), total projectile roll is only about 45 degrees (1/8 revolution). Assume for illustration purposes that the trim vector orientation at the muzzle is up, as depicted in Figure 22.

After 1/4 yaw cycle, the projectile reaches first maximum yaw, but the trim vector has only rotated about 10 to 12 degrees. Figure 23 shows the relative orientations of the three vectors that sum to produce the projectile first maximum yaw. Notice that for this arbitrary case, the effect of the trim vector has been to actually increase the total angle of attack magnitude over what it would have been without any trim vector. Next, 1/2 yaw cycle later, the projectile achieves its point of second maximum yaw. By this point, the trim vector has rotated approximately 30 to 35 degrees from its original orientation. Note in the resultant vector of Figure 24 how the trim vector now causes a net decrease in the total yaw angle relative to total yaw in the absence of trim.

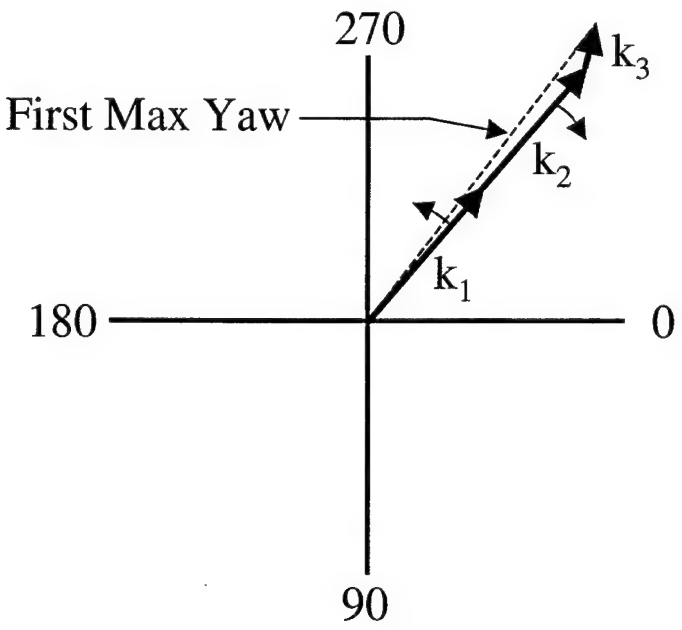

Figure 23. Tricyclic Motion Model at First Maximum Yaw With Trim.

Analysis of yaw data showed evidence of the presence of a trim vector of varying magnitude for four of the five shots. This was evidenced both by the reduction code's calculation of a finite trim angle in both the linear theory and 6-DOF reductions and by the characteristic stepping of the yaw peaks in the angular fits. Computed trim angle values for all shots are presented in Table 3. Agreement is

good between the independent calculations of linear theory and the 6-DOF calculations. Inclusion of the computed trims in the angular fits resulted in improved fit errors in all cases except Shot 2.

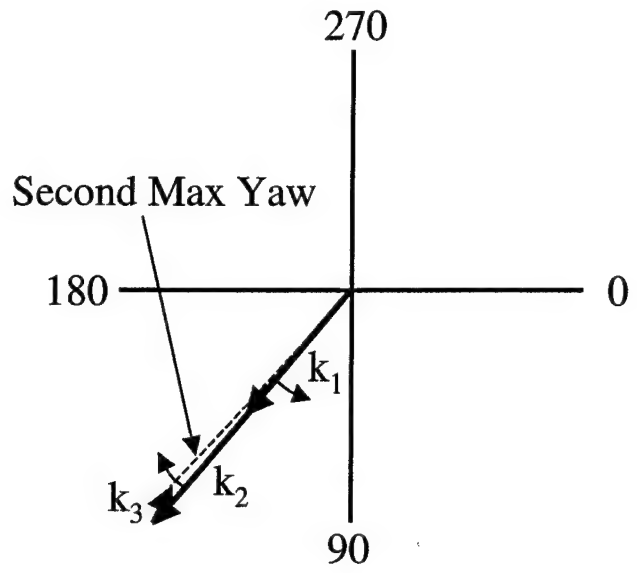

Figure 24. Tricyclic Motion Model at Second Maximum Yaw With Trim.

Table 3. Calculated Trim Angles

Shot No.	Linear Theory Trim (deg)	6-DOF Trim (deg)
1	0.114	0.136
2	0.001	0.038
3	0.257	0.264
4	0.108	0.171
5	0.162	0.149

There are several possible origins of trim, including mass or aerodynamic asymmetry. A mass asymmetry could be introduced by a loose internal part or by a manufacturing inaccuracy. However, the M831A1 has no internal parts that could become loose. Moreover, given the strict M831A1 manufacturing tolerances, the current state of the art in machining technology, and the physical size of the projectile, a mass asymmetry is considered very unlikely. The possibility of an aerodynamic asymmetry is more likely. In some cases as a result of launch, minor damage may exist on one side of a projectile. Other possible

explanations could be offered, including occasions when an obturator band stays on the round but protrudes into the free stream more on one side of the projectile than another. It is noted that there is no evidence to confirm any particular explanation for the presence of aerodynamic trim. Despite this, the data substantiate that trim exists.

Another important result from the yaw data was their characteristic growth or damping. Table 4 shows the yaw trend with range, along with the root mean squared yaw level. From the table, note that three of the five shots displayed some level of yaw growth with range. Typically, when roll and yaw frequencies are within 25% of each other, coupling occurs, with a resultant increase in yaw (Whyte et al., 1994). Over the range of instrumented trajectory, the roll frequencies were well below the yaw frequencies in all cases. Furthermore, the radar data of Whyte et al. show that roll-yaw amplification does not normally occur until after 1000 meters for the M831A1. Hence, the yaw growth observed here cannot be attributed to roll-yaw coupling. Rather, the yaw-damping characteristics are most plausibly attributed to a marginal pitch-damping moment coefficient, as described in the next section. It is important that although yaw growth was observed for several rounds, these rounds did *not* necessarily become unstable down range. Also, no correlations are evident between the observed damping trend and the yaw level.

Table 4. Yaw Damping Trends

Shot	Damping Trend	Root Mean Squared Yaw (deg^2)
1	Growing	1.21
2	Neutral	6.51
3	Growing	0.66
4	Growing	2.89
5	Damping	0.94

3.4 Aerodynamic Coefficients

The analysis performed with the ARFDAS code proceeds in several steps. First, a best fit is obtained to the measured position and angle data via the linearized equations of motion. From this, aerodynamic coefficients are obtained. Next, these data are used as initial input for the full 6-DOF computations. Here, the aerodynamic coefficients are adjusted to provide the best data fit as computed with the full 6-DOF equations of motion. Presented next are the aerodynamic coefficient data resulting from the full 6-DOF analysis.

First, zero-yaw drag coefficient, C_{X0}, is plotted in Figure 25. Since drag is easily and accurately measured, all five individual data points fall on a line with minimal scatter.

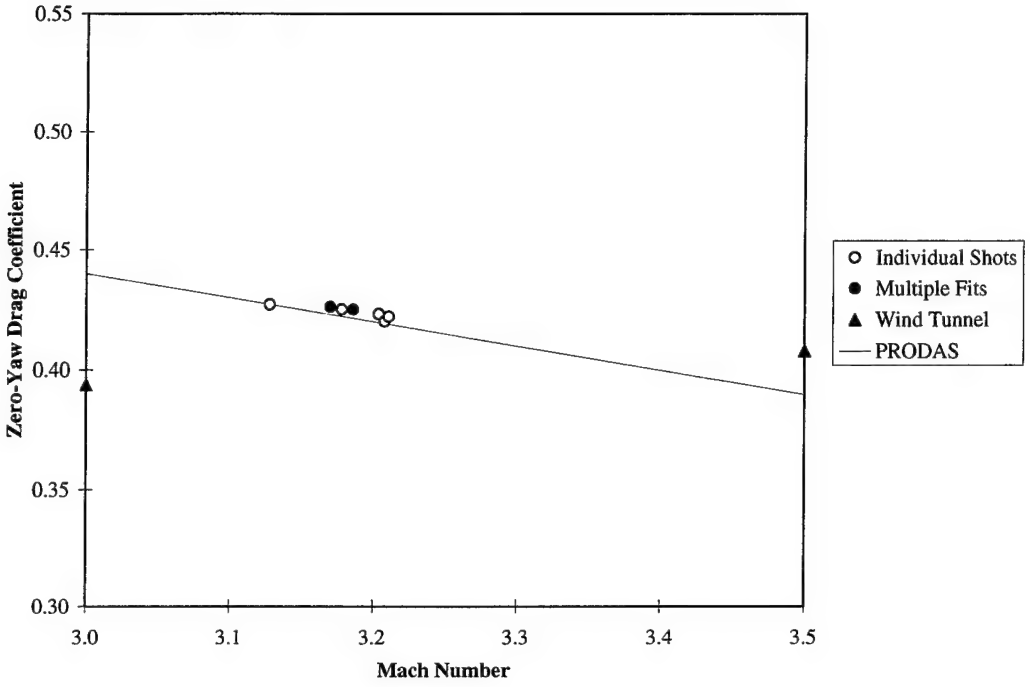

Figure 25. Zero-yaw Drag Versus Mach Number.

All shots were fired without tracers, and thus, the drag coefficients determined will likely be a few percent higher than those obtained from any other experiments in which traced rounds were fired. The solid circle data points represent multiple fits in which the reduction routine is constrained to compute a single value of drag coefficient for the data of multiple shots. In the case of zero-yaw drag, the coefficient value is not enhanced by the multiple fit capability since the coefficients obtained from the individual shots are already very accurate. Also note that the data are in excellent agreement with predicted values computed by the PRODAS design code. Two wind tunnel data points are also shown for comparison (Farina, 1997). Although not plotted, the first and second nonlinear drag components were obtained with greater than anticipated accuracy. This was possible because of several shots that exhibited moderate to high yaw levels. The average value determined for $C_{X\alpha 2}$ was 29.8 with a probable error of just 2.1%, and for $C_{X\alpha 4}$, it was -530 with a probable error of 6.2%. These values were previously unknown and are somewhat different from predicted values.

Pitching moment coefficient, $C_{m\alpha}$, is plotted in Figure 26. As in the case of drag, the individual data points show little scatter, and both the PRODAS-predicted values and wind tunnel data match very well with the experimental data. The value of $C_{m\alpha}$ for Shot 3 was -1.54 and was the most different from the multiple fit values. This can be attributed to the low yaw in this shot, resulting in a less accurate determination of $C_{m\alpha}$. Note that the pitching moment coefficient values are much smaller than are typical for a statically stable projectile because of the projectile's relatively lower static margin. The cubic pitching moment coefficient was also determined with a 10% probable error as -5.2.

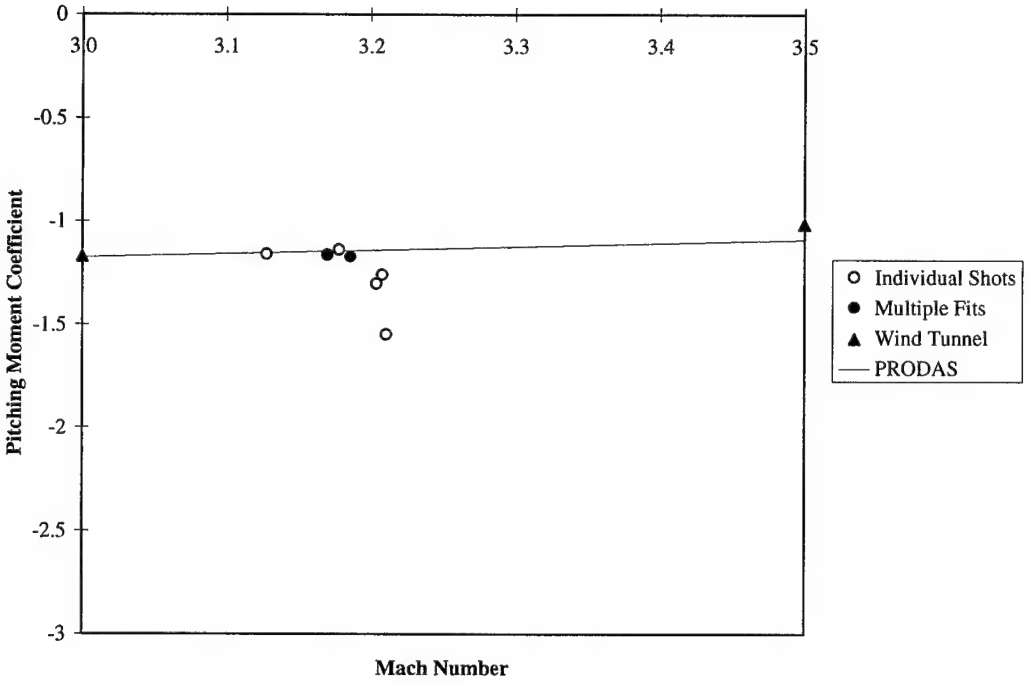

Figure 26. Pitching Moment Coefficient Versus Mach Number.

Normal force coefficient, $C_{N\alpha}$, is plotted in Figure 27. Only multiple fit values of the coefficient are plotted since individual shot data produced fairly significant scatter. This is because accurate calculation of the coefficient is a function of the amount of projectile swerve (center of gravity motion). Three shots in particular resulted in poor $C_{N\alpha}$ values. All three had swerve arm magnitudes that were significantly smaller than those of the other two shots, thus leading to more error in these values. As with all coefficients, the most accurately computed values are those resulting from the multiple fit reductions. Again, both wind tunnel data and PRODAS predictions match well with the experimental free flight numbers.

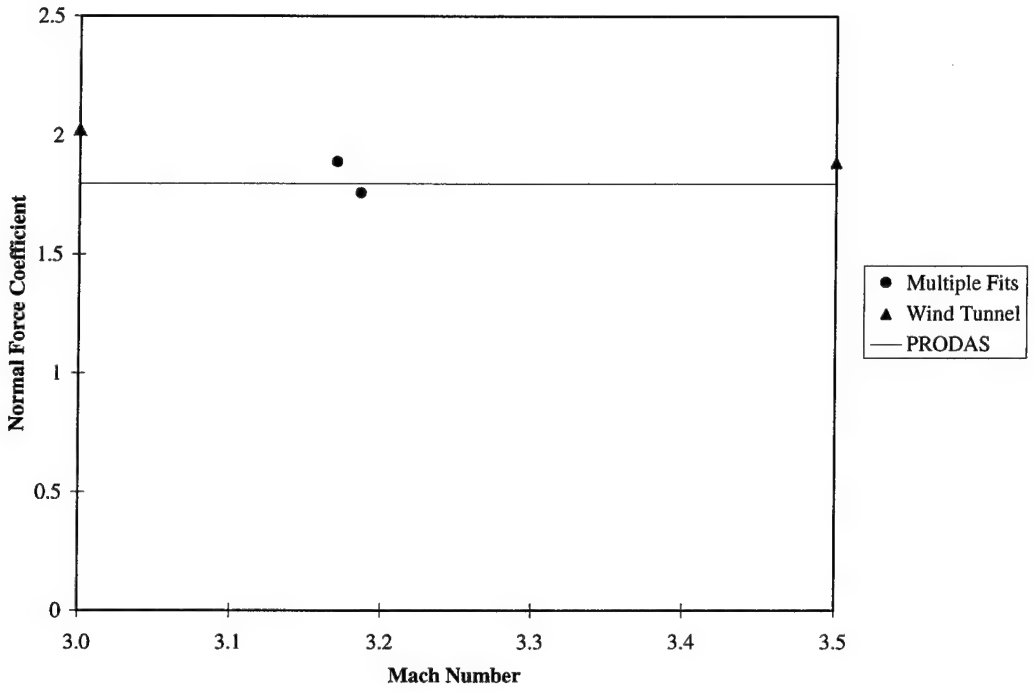

Figure 27. Normal Force Coefficient Versus Mach Number.

Finally, Figure 28 plots multiple fit values of pitch-damping moment coefficient, C_{mq}. Accurate computation of C_{mq} depends upon the yaw level, the number of complete yaw cycles measured, and the amount of damping that occurs. In general, the greater the yaw magnitude and the more cycles that are measured, the more accurate the pitch-damping coefficient will be. However, even for high yaw shots in which several complete yaw cycles are measured, if the overall *change* in yaw level with range is small, then damping characteristics are very difficult to extract accurately. This was the case with the high yaw shot of the current experiment; despite high yaw and approximately 3.5 yaw periods measured, the yaw level stayed nearly constant with range. In other words, damping was neutral, and thus, an accurate pitch-damping moment coefficient was indeterminate. The same type of phenomenon was observed with the three other shots that displayed marginal pitch-damping characteristics. In all three cases, low yaw level or a minimal *change* in yaw with range (marginal damping) or a combination of both resulted in C_{mq} values with high probable errors. One shot produced a calculated C_{mq} of -12.4 with low yaw, but the amount of damping present allowed a somewhat reasonable probable error of 25%. This data point is not plotted, but note that this value is consistent with the PRODAS prediction. Even the multiple fit values of C_{mq} resulted in very high probable errors—again, because the relative amount of damping was very small. This fact provides further confirmation that an accurate value for the pitch-damping moment coefficient is not possible from the current data set. However, the

analysis clearly indicates that marginal pitch damping exists, and therefore, the PRODAS-predicted value might be optimistic.

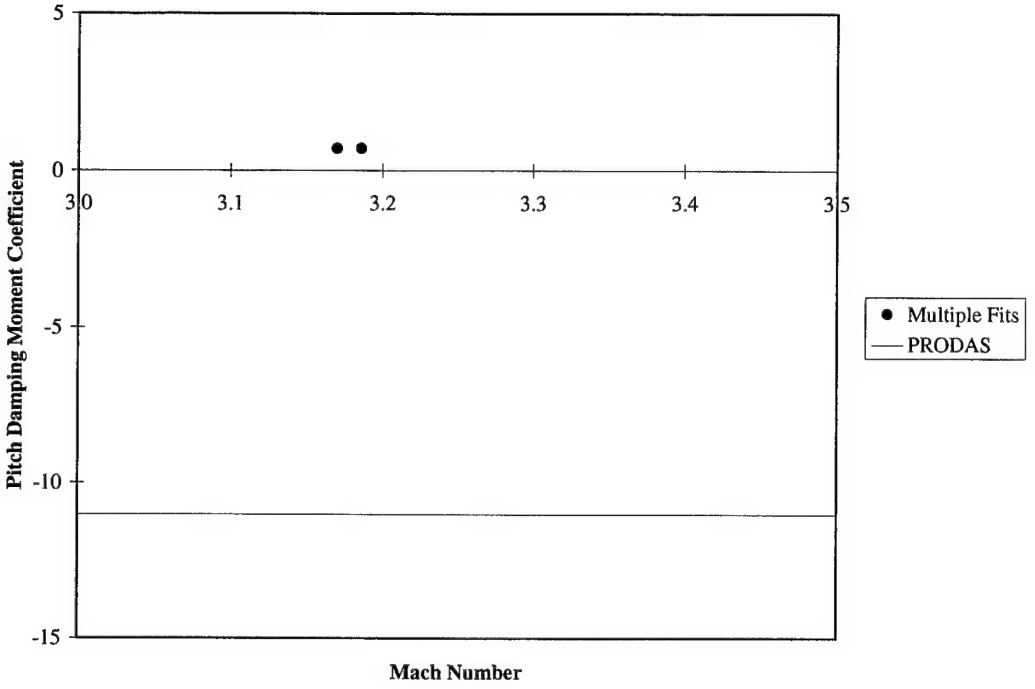

Figure 28. Pitch-Damping Moment Coefficient Versus Mach Number.

Table 5 presents a summary of aerodynamic coefficient values determined from multiple fit data analysis, together with their associated probable errors. The nonlinear coefficient terms ($C_{X\alpha 2}$, $C_{X\alpha 4}$, $C_{m\alpha 3}$) were determined from the two shots with the highest yaw levels. The PRODAS-predicted values of $C_{\ell p}$ and $C_{\ell 0}$ (-0.045 and 0.0024, respectively) were used to determine roll, except for Shot 5, for which the actual measured roll data were used.

4. Conclusions

The data and analysis presented in this report are the result of the first free flight, highly instrumented and analyzed experiment conducted on the M831A1 training projectile. This work is a significant step toward a comprehensive understanding of the complex aerodynamic phenomena that lead to the performance characteristics of this projectile.

Table 5. Aerodynamic Coefficients

Coefficient	Value	Probable Error (percent)
Drag		
Zero Yaw (C_{X0})	0.425	0.1
Squared Component ($C_{X\alpha 2}$)	29.8	2.1
Quad Component ($C_{X\alpha 4}$)	-530	6.2
Pitching Moment		
Linear ($C_{m\alpha}$)	-1.17	0.9
Cubic Component ($C_{m\alpha 3}$)	-5.2	9.9
Normal Force	1.8	3.8
Pitch-Damping Moment	1	**

**Probable error too high for reliable value

Although the integrity of the roll data was less than desired, the gaps were filled by careful hand measurement of all shadowgraphs. This resulted in an excellent qualitative assessment of the early roll history. All five rounds exhibited very little roll over the measured trajectory (on the order of 120 degrees in 200 meters). This is because a less-than-optimum roll moment is present. This phenomenon is also visible in the variability in the roll from round to round. Some projectiles rolled approximately 1/2 turn, while others rolled less than 1/4 turn over the same range. Also, projectile "roll up" is hindered by a high rotational inertia. Accurate values of $C_{\ell p}$ and $C_{\ell 0}$ were not obtained, although $C_{\ell 0}$ is believed to be in the range of 0.0010 to 0.0016, based upon empirical analyses. A more accurate value of $C_{\ell 0}$ could probably be determined in future investigation, given the knowledge gained from the current experiment.

Yawing motion also displayed variability. The first maximum yaw of one shot reached beyond 9 degrees. Another shot experienced moderate yaw level, and the remaining three experienced relatively low levels. The source of the yaw level imparted to the projectile is the launch dynamics, which are a result of the in-bore dynamics. A detailed study of in-bore dynamics is progressing for the purpose of understanding the variables that have the most significant impact on launch dynamics for the M831A1.

Four of five shots exhibit "stepping" in the total yaw with range. This phenomenon is the result of trim. This is believed to be caused by an aerodynamic asymmetry, although an exact source has not been isolated. Accurate free flight values for drag, pitching moment, and normal force

coefficients were determined, along with nonlinear components of both drag and pitching moment. The nonlinear effect of yawing on drag force was under-predicted by PRODAS. The pitch-damping moment coefficient was not determined to within the desired accuracy. However, pitch damping of the M831A1 is clearly marginal, as evidenced not only by the coefficient values but also by the damping characteristics observed in the experiment. This could serve as a potential explanation for the occasional anomalous rounds observed by the user. However, the data from the current experiment are far too few, as yet, to provide insight into the possible need for a CCF modification.

5. Recommendations

The results of the current study have resulted in significantly greater insight into the M831A1's aerodynamic characteristics. However, the knowledge base is still incomplete. Further study is needed to obtain more information. Although the data analysis of this very small number of shots produced accurate and informative results, the results cannot necessarily be considered representative of the M831A1. Confidence in these conclusions will be greatly enhanced by further detailed experiments. Regardless of the M831A1's current TID performance, such data will prove valuable in both the present and future development of the projectile.

In particular, an accurate $C_{\ell 0}$ value will shed more light on down-range roll profiles and steady state roll rates. If the roll moment is inadequate, as proposed here and as concluded by Whyte et al. (1994), methods of increasing this moment at minimal cost can and should be addressed. Equally important, a close examination of the projectile's damping characteristics is needed.

As a first step toward the investigation of increasing roll moment, ARDEC has developed an alternate stabilizer design. The new design employs two additional torque-generating stabilizer slots and increases the cant angle of all eight slots (Farina 1999). This new stabilizer has already been tested in the wind tunnel and is scheduled for free flight evaluation in the near future.

Finally, ARL has proposed an alternate stabilizer design, shown with standard cartridge components in Figure 29. This design uses canted fins instead of slots to induce roll and represents a more radical departure from the current configuration. The overall wetted area used to induce roll is significantly larger here than in the current design. Additionally, such a concept could possibly increase both static and pitch-damping moments, although this would require confirmation through careful analysis. Investigation of this and other stabilizer

concepts is recommended while performance, complexity, and cost are considered.

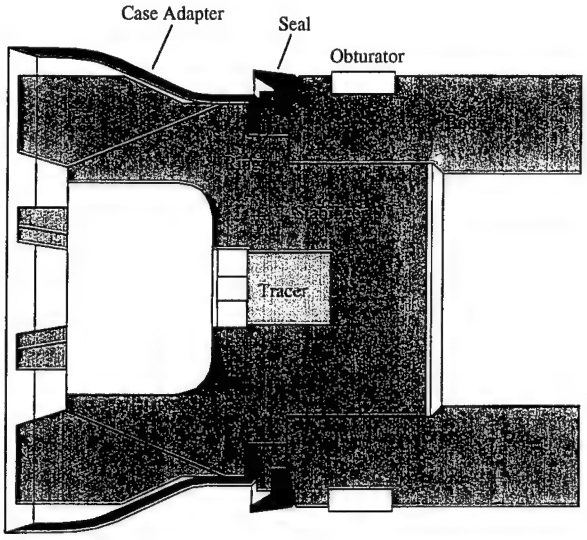

Figure 29. ARL Alternate Stabilizer Concept.

References

Dohrn, R., Private communication, Alliant Techsystems, Hopkins, MN, December 1999.

Durkin, P., Private communication, Aberdeen Test Center, Aberdeen Proving Ground, MD, December 1999.

Farina, A., Supersonic wind tunnel data (unpublished), U.S. Army Research, Development, and Engineering Center, Picatinny Arsenal, NJ, April 1997.

Farina, A., "M831A1 Modeling and Simulation Wind Tunnel Test," briefing presented at the U.S. Army Research Laboratory, Aberdeen Proving Ground, MD, November 1999.

Hathaway, W., Private communication, Arrowtech Associates, South Burlington, VT, December 1999.

Murphy, C.H., "Free Flight Motion of Symmetric Missiles," BRL-MR-1216, U.S. Army Ballistic Research Laboratory, Aberdeen Proving Ground, MD, July 1963.

Whyte, R., W. Hathaway, and J. Groth, "Aeroballistic Characteristics of the M831A1 Determined from Doppler Radar Data," technical report, Arrowtech Associates, South Burlington, VT, August 1994.

INTENTIONALLY LEFT BLANK

APPENDIX A

PITCH-YAW PLOTS, SHOTS 2 THROUGH 5, AND COMPLEX PLOTS, ALL SHOTS

INTENTIONALLY LEFT BLANK

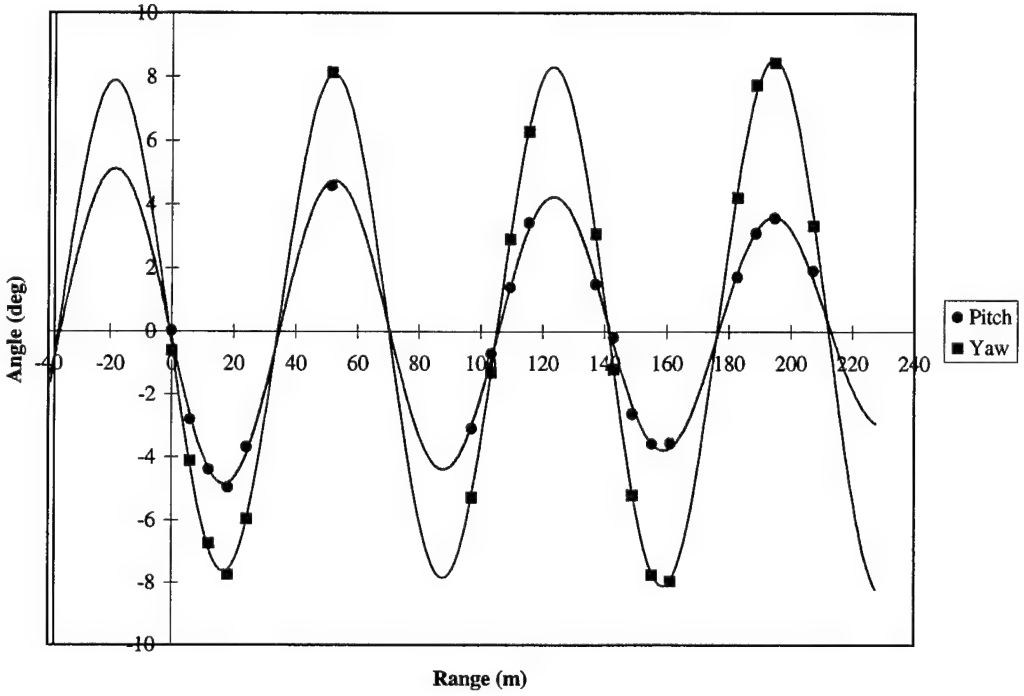

Figure A-1. Pitch and Yaw Versus Range, Shot 2.

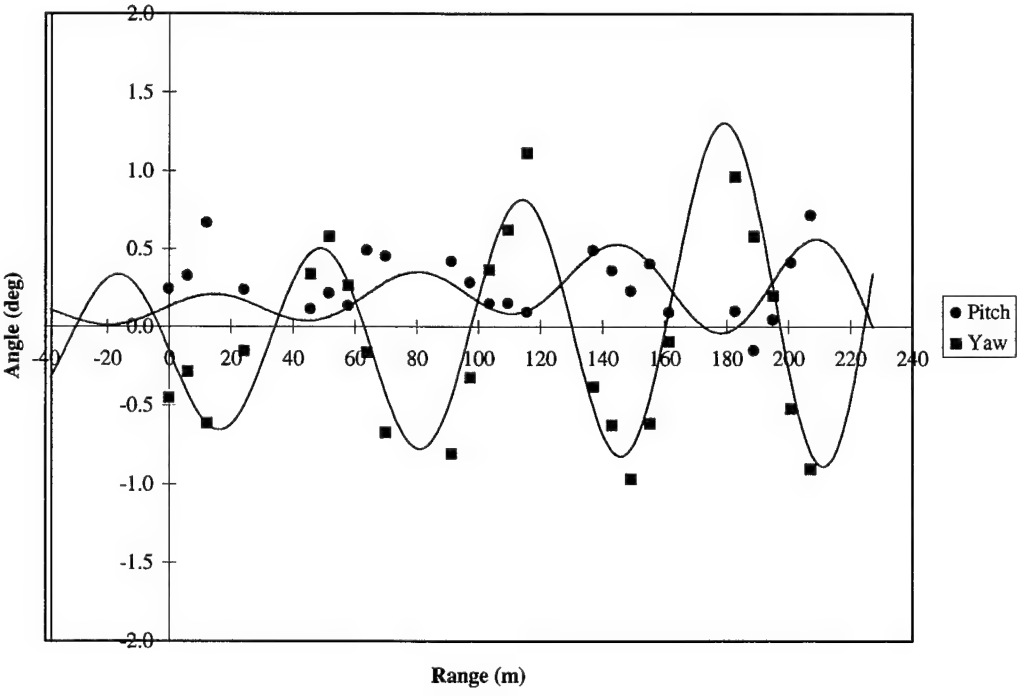

Figure A-2. Pitch and Yaw Versus Range, Shot 3.

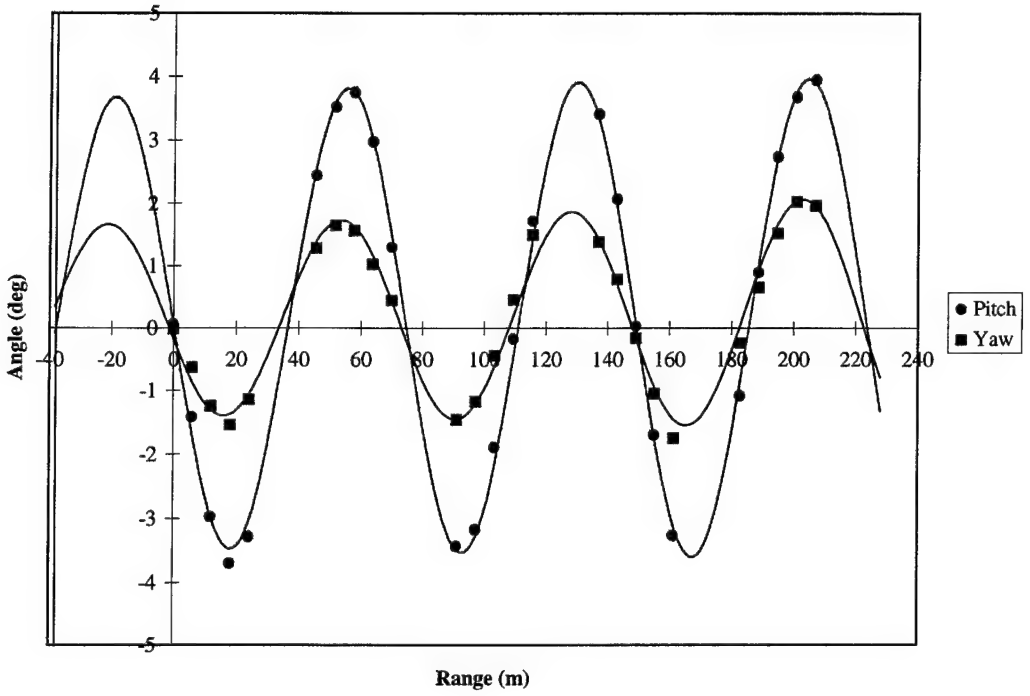

Figure A-3. Pitch and Yaw Versus Range, Shot 4.

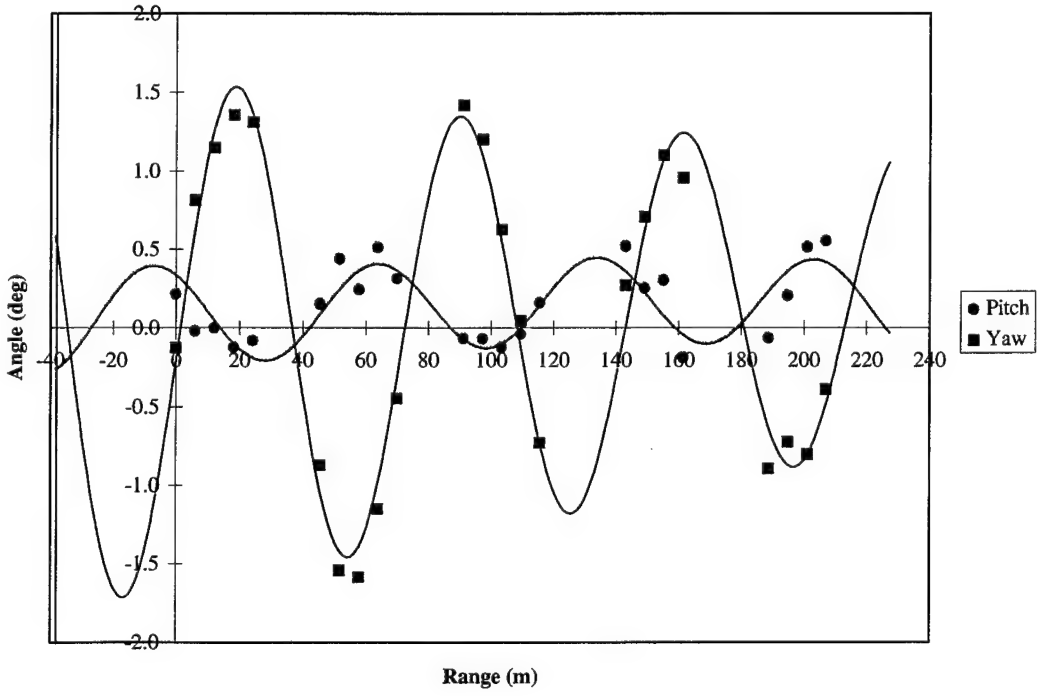

Figure A-4. Pitch and Yaw Versus Range, Shot 5.

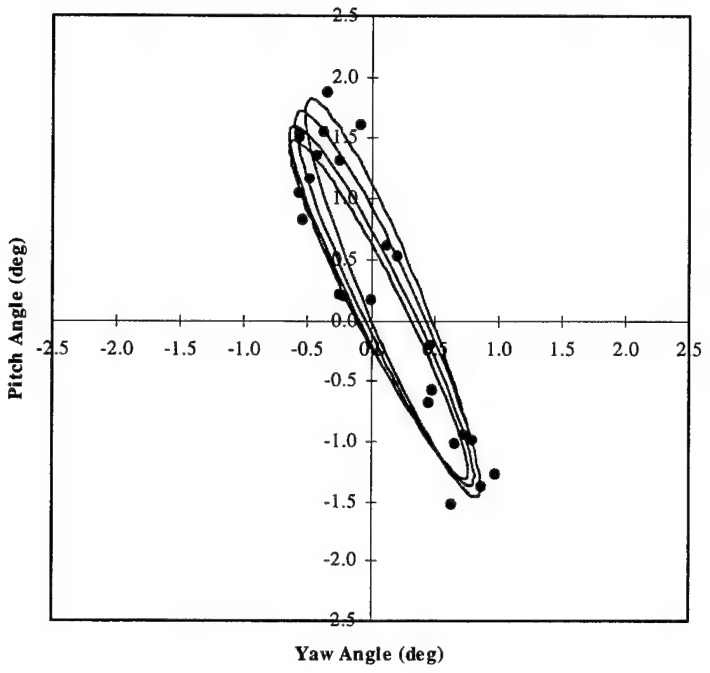

Figure A-5. Pitch Versus Yaw, Shot 1.

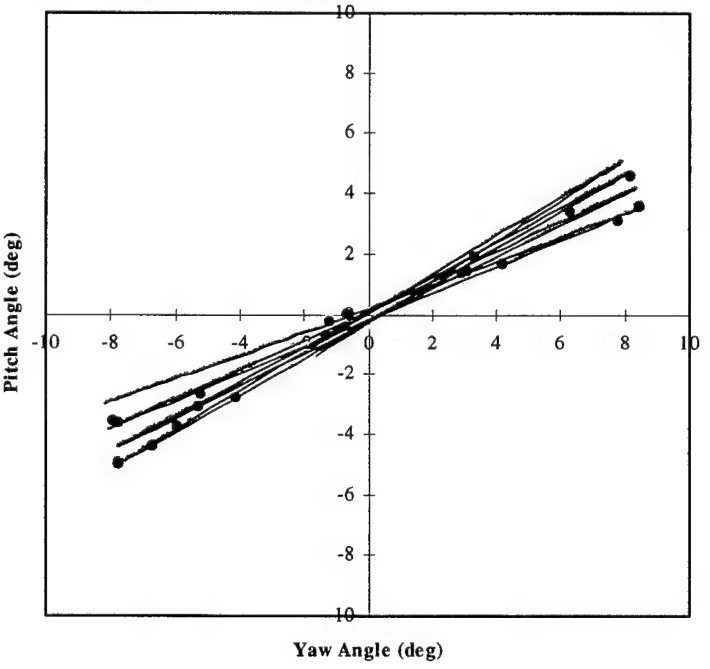

Figure A-6. Pitch Versus Yaw, Shot 2.

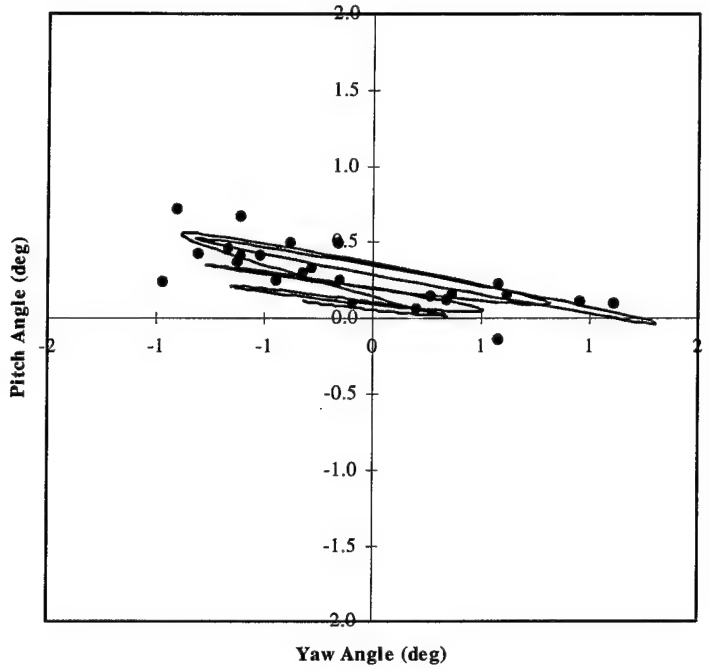

Figure A-7. Pitch Versus Yaw, Shot 3.

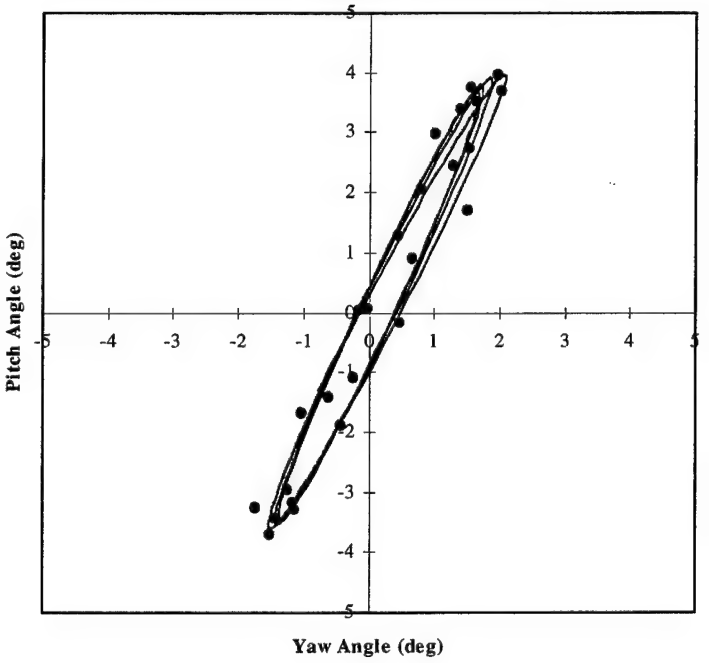

Figure A-8. Pitch Versus Yaw, Shot 4.

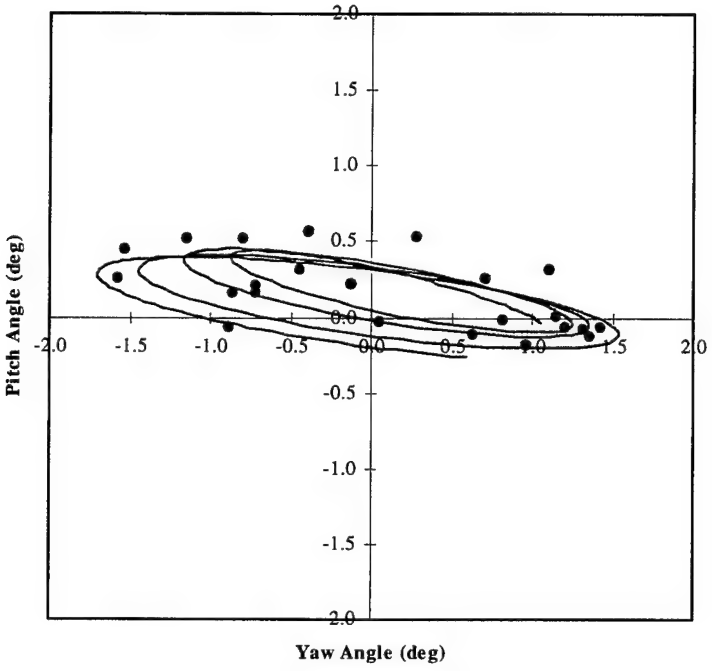

Figure A-9. Pitch Versus Yaw, Shot 5.

INTENTIONALLY LEFT BLANK

NO. OF COPIES ORGANIZATION

1 ADMINISTRATOR
DEFENSE TECHNICAL INFO CTR
ATTN DTIC OCA
8725 JOHN J KINGMAN RD
STE 0944
FT BELVOIR VA 22060-6218

1 DIRECTOR
US ARMY RSCH LABORATORY
ATTN AMSRL CI AI R REC MGMT
2800 POWDER MILL RD
ADELPHI MD 20783-1197

1 DIRECTOR
US ARMY RSCH LABORATORY
ATTN AMSRL CI LL TECH LIB
2800 POWDER MILL RD
ADELPHI MD 207830-1197

1 DIRECTOR
US ARMY RSCH LABORATORY
ATTN AMSRL D D SMITH
2800 POWDER MILL RD
ADELPHI MD 20783-1197

1 DIRECTOR
US ARMY RSCH LABORATORY
ATTN AMSRL CP CA D SNIDER
2800 POWDER MILL RD
ADELPHI MD 20783-1197

6 ALLIANT TECHSYSTEMS INC
ATTN R BECKER L OSGOOD
T HUNGERFORD
R PETERSON A SKEATES
T THOMPSON
MN21 2055
TCAAP BUILDING 104
HIGHWAY 10 WEST
NEW BRIGHTON MN 55112

7 ALLIANT TECHSYSTEMS INC
ATTN C AAKHUS
C CANDLAND
R DOHRN (5 CYS)
M JANTSCHER
600 SECOND STREET NE
HOPKINS MN 55343

NO. OF COPIES ORGANIZATION

4 CDR US ARMY TACOM ARDEC
ATTN AMSTA AR QAC T
A CHAN (2 CYS)
J DEMARIA M BOMUS
BLDG 65 SOUTH
PICATINNY ARSENAL NJ 07806-5000

7 CDR U S ARMY ARDEC
ATTN AMSTA AR CCH B
J CANELA W CRAMER
P DONADIO J KOSTKA
L MANOLE W RICE
P VALENTI
BLDG 65 SOUTH
PICATINNY ARSENAL NJ 07806-5000

1 CDR U S ARMY ARDEC
ATTN AMSTA AR FSF T
A FARINA
BLDG 382
PICATINNY ARSENAL NJ 07806-5000

5 CDR U S ARMY ARDEC
ATTN AMSTA AR CCH A
R CARR J GRAU
G MALEJKO S MUSALLI
M PALATHINGAL
BLDG 65 SOUTH
PICATINNY ARSENAL NJ 07806-5000

1 U S ARMY TRADOC
DIR OF TRAINING & DOCTRINE DEV
DOCTRINE DIVISION
ATTN ATZK TDD ORSA A POMEY
RM 202 HARRIS HALL
BLDG 2368
FT KNOX KY 40121-5000

3 PRIMEX TECHNOLOGIES INC
ATTN V BURRELL
P RADCZENKO A SAITTA
10101 9TH STREET NORTH
ST PETERSBURG FL 33716

1 PRIMEX TECHNOLOGIES
ATTN G HOGSETT
PO BOX 127
RED LION PA 17356-0127

NO. OF COPIES ORGANIZATION

2 CDR U S ARMY MUNITIONS
&ARMAMENTS CMD
ATTN SOSMA PRC T
B DAVIES
D PORTERFIELD
1 ROCK ISLAND ARSENAL
ROCK ISLAND IL 61299-5500

3 ARROWTECH ASSOCIATES
ATTN R WHYTE
W HATHAWAY
A HATHAWAY
1233 SHELBURNE RD
SUITE D8
SOUTH BURLINGTON VT 05403

ABERDEEN PROVING GROUND

2 DIRECTOR
US ARMY RSCH LABORATORY
ATTN AMSRL CI LP (TECH LIB)
BLDG 305 APG AA

3 DIRECTOR
US ARMY RSCH LABORATORY
ATTN AMSRL WM B A HORST
E SCHMIDT W CIEPIELA
BLDG 4600

1 DIRECTOR
US ARMY RSCH LABORATORY
ATTN AMSRL WM BA R MCGEE
BLDG 4600

14 DIRECTOR
US ARMY RSCH LABORATORY
ATTN AMSRL WM BC D LYON
M BUNDY G COOPER
T ERLINE B GUIDOS
P PLOSTINS J NEWILL
J SAHU D WEBB
K SOENCKSEN (3 CYS)
P WEINACHT A ZIELINSKI
BLDG 390

2 DIRECTOR
US ARMY RSCH LABORATORY
ATTN AMSRL WM BC
J GARNERV OSKAY
BLDG 740

NO. OF COPIES ORGANIZATION

1 DIRECTOR
US ARMY RSCH LABORATORY
ATTN AMSRL WM BD B FORCH
BLDG 4600

1 DIRECTOR
US ARMY RSCH LABORATORY
ATTN AMSRL-WM BF J LACETERA
BLDG 390

1 DIRECTOR
US ARMY RSCH LABORATORY
ATTN AMSRL WM MD VIECHNICKI
BLDG 4600

3 DIRECTOR
US ARMY RSCH LABORATORY
ATTN AMSRL WM MB B FINK
W DRYSDALE C HOPPEL
BLDG 4600

1 DIRECTOR
US ARMY RSCH LABORATORY
ATTN AMSRL WM T B BURNS
BLDG 4600

1 DIRECTOR
US ARMY RSCH LABORATORY
ATTN AMSRL WM TC R COATES
BLDG 390A

REPORT DOCUMENTATION PAGE

Form Approved OMB No. 0704-0188

1. AGENCY USE ONLY *(Leave blank)*	2. REPORT DATE	3. REPORT TYPE AND DATES COVERED
	November 2000	Final

4. TITLE AND SUBTITLE

Aerodynamics of the 120-mm M831A1 Projectile: Analysis of Free Flight Experimental Data

5. FUNDING NUMBERS

PR: 1L162618AH80

6. AUTHOR(S)

Soencksen, K.P.; Newill, J.F.; Plostins, P. (all of ARL)

7. PERFORMING ORGANIZATION NAME(S) AND ADDRESS(ES)

U.S. Army Research Laboratory
Weapons & Materials Research Directorate
Aberdeen Proving Ground, MD 21005-5066

8. PERFORMING ORGANIZATION REPORT NUMBER

9. SPONSORING/MONITORING AGENCY NAME(S) AND ADDRESS(ES)

U.S. Army Research Laboratory
Weapons & Materials Research Directorate
Aberdeen Proving Ground, MD 21005-5066

10. SPONSORING/MONITORING AGENCY REPORT NUMBER

ARL-TR-2307

11. SUPPLEMENTARY NOTES

12a. DISTRIBUTION/AVAILABILITY STATEMENT

Approved for public release; distribution is unlimited.

12b. DISTRIBUTION CODE

13. ABSTRACT *(Maximum 200 words)*

The 120-mm M831A1 projectile is a low-cost training projectile used by U.S. armor troops. For the last several years, program managers have received feedback from the users that in some cases, M831A1 impact performance did not appear consistent with the current M831A1 computer correction factor. Based on this information, a low-scale but in-depth experimental analysis of the projectile was conducted to assess its aero-ballistic qualities and hopefully identify any potential issues that could affect accuracy performance. The work was conducted by the U.S. Army Research Laboratory at the Transonic Experimental Facility. Although the projectile has undergone fairly extensive target impact dispersion (TID), radar, and wind tunnel testing, this study presents the first spark range data and detailed free-flight aero-ballistic analysis for the M831A1.

Roll data were measured via roll pins for the computation of roll-related coefficients. All rounds exhibited very little roll over the measured trajectory, mostly because of a very small roll moment. Yaw magnitudes displayed variability, and several shots had at least moderate levels. The source of the yaw levels imparted to the projectiles was the launch dynamics, and a detailed study of in-bore dynamics is in progress. Most shots exhibited a "stepping" motion in plots of total yaw versus range. This phenomenon is the result of trim, which is believed to be caused by an aerodynamic asymmetry. A source of the trim has not been isolated. Accurate free-flight drag and pitching moment coefficients were computed on the basis of the measured trajectories. Pitch-damping characteristics were marginal.

Although the M831A1 currently performs within acceptable TID standards, further experimental work is recommended, as well as a study of possible stabilizer design modifications.

14. SUBJECT TERMS		15. NUMBER OF PAGES
aerodynamics	M831A1	45
experimental	projectile	16. PRICE CODE

17. SECURITY CLASSIFICATION OF REPORT	18. SECURITY CLASSIFICATION OF THIS PAGE	19. SECURITY CLASSIFICATION OF ABSTRACT	20. LIMITATION OF ABSTRACT
Unclassified	Unclassified	Unclassified	